Information Sciences 544 (2021) 395–414

Contents lists available at ScienceDirect

Information Sciences

journal homepage: www.elsevier.com/locate/ins

Fault tolerant sampled-data $\mathcal{H}_\infty$ control for networked control systems with probabilistic time-varying delay

Fang Fang [a], Haotian Ding [a], Yajuan Liu [a,*], Ju H. Park [b,*]

[a] School of Control and Computer Engineering, North China Electric Power University, Beijing 102206, PR China
[b] Department of Electrical Engineering, Yeungnam University, 280 Daehak-Ro, Kyongsan 38541, Republic of Korea

ARTICLE INFO

Article history:
Received 19 December 2019
Received in revised form 17 August 2020
Accepted 18 August 2020
Available online 29 August 2020

Keywords:
Probabilistic time delays
Networked control systems
Actuator faults
Extended reciprocally convex matrix inequality
Vehicle active suspension

ABSTRACT

In this study, the problem of fault-tolerant sampled-data $\mathcal{H}_\infty$ control for a networked control system with random time delays and actuator faults is investigated. Stochastic variables conforming with the Bernoulli distribution are considered to depict random time delays. A state feedback sampled-data controller is designed to ensure the asymptotical stability and $\mathcal{H}_\infty$ performance of the resulting closed-loop system. By applying the Lyapunov–Krasovskii stability theory and the reciprocally convex combination lemma, a stability criterion for a random time-varying delay system is developed that guarantees the designed controller can satisfy the requirements of stability and maneuverability. The desired controller gain is then found based on the linear matrix inequalities. Finally, as a real application, a quarter-vehicle suspension system model is provided to demonstrate the benefits and validity of the proposed control law.

1. Introduction

Networked control systems (NCSs) have the capability to connect sensors, controllers, and plants over a communication network [1]. In addition, owing to the advantages of low cost, good stability, flexibility, and easy maintenance [2,3], NCSs have been widely applied to numerous practical engineering systems [4–6], such as spacecraft, vehicle suspensions [5], and manufacturing plants [6]. In particular, various disturbances are inevitable in many practical engineering systems, which might lead to system instability and a performance degradation. It is therefore essential to determine a method to reduce and eliminate the impact of interference. One effective approach to reduce the impact of interference and optimize the system performance is the use of $\mathcal{H}_\infty$ control. The main object of $\mathcal{H}_\infty$ control is to design a controller such that the resulting closed-loop system is asymptotically stable, and controlled outputs with an external input are lower than the prescribed performance of $\mathcal{H}_\infty$. During the past few years, several findings on $\mathcal{H}_\infty$ control have been reported [7–11]. For instance, a disturbance attenuation problem with hard time-domain constraints was solved using an $\mathcal{H}_\infty$ method [7]. A novel finite-horizon $\mathcal{H}_\infty$ control method for stochastic nonlinearity systems was designed [9]. In addition, the Youla parameterization approach was applied to the design of an $\mathcal{H}_\infty$ controller for uncertain polytopic systems [11]. In addition, some $\mathcal{H}_\infty$ control designs for NCSs have been obtained [12–15]. A finite frequency controller was designed for a vehicle suspension system within the frequency domain [12]. By using a robust regularized least squares method, a new controller design approach was derived [14]. An improved $\mathcal{H}_\infty$ performance index was also derived through an indefinite quadratic performance function [15].

* Corresponding author.
E-mail addresses: yajuan.liu.12@gmail.com (Y. Liu), jessie@ynu.ac.kr (J.H. Park).

https://doi.org/10.1016/j.ins.2020.08.063
0020-0255/

As is well known, most controllers in practical systems are designed by employing digital technology because the connection among the controllers, sensors, and actuators in practical implementations is realized through digital signals [16]. Thus, a sampled-data control approach has been widely studied because it can be directly used in the design of a digital controller for a continuous-time system [17–20]. For example, in [17], an $\mathcal{H}_\infty$ controller for vehicle suspensions using sampling was investigated. In addition, the authors proposed a sampled-data fuzzy control method for NCSs [19]. In general, there are three approaches investigating a sampled-data control design: a discretization approach, an impulsive model approach, and an input delay approach. The first method relies on lifting techniques to transform the system into an equivalent discrete system. The second method is realized by solving differential Riccati equations with jumps. Finally, the last approach is expressed as a delay control between two-time sampling intervals. By utilizing the input delay method, traditional sampled-data systems are transformed into time-varying delay systems. In contrast with the first two methods, the merit of the input delay approach is that the sampling distances do not need to be constant [21–23]. Therefore, applying the input delay approach into the design of the networked control system (NCS), in which the NCS is transformed into a time-delay system, is significant. The Lyapunov–Krasovskii functional (LKF) approach is then applied to establish the stability conditions, and many novel matrix inequalities have been proposed [24–30]. Among these methods, the reciprocally convex combination lemma (RCCL) achieves an accurate convex inequality by combining the different non-convex terms in an expression, which has been proved to be an effective way to improve the stability criteria [31]. This method combines well with other integral inequality methods and can provide less conservative results for the NCSs.

In addition, it is noteworthy that the sampled-data control methods mentioned above are obtained under deterministic sampling [17,19]. Nevertheless, a time delay appears in a probability mechanism owing to various external random factors or communication distractions in a practical control system [32–34]. Hence, the probability sampling mechanism must be considered. And many studies utilizing probabilistic sampling effects have been realized [35–37]. In comparison with deterministic sampling, a larger sampling interval has been obtained [35]. By employing a stochastic analysis technique, sufficient conditions have been developed to satisfy the performance constraint of a dynamic system [36]. In addition, a complex network system with randomly varying delays has been a concern in this field [37].

The aforementioned methods are realized when the systems are well established through the application of actuators and sensors [35]. However, the structure of the system is not static because faults are inevitable and unpredictable, which can cause instability and degrade the performance [38]. Thus, it is necessary to design a controller that can tolerate system faults. Therefore, a fault-tolerant control design has received substantial attention, and some interesting results have been obtained [39–46]. For instance, a fault-tolerant control strategy was proposed for a spacecraft system with actuator faults [41]. The authors in [43,44] presented two types of reliable fuzzy fault-tolerant control methods for NCSs. In [42], a resilient reliable problem for practical systems with deterministic actuator faults was investigated.

Based on the above discussions, various external random factors, communication distractions, and actuator faults are inevitable in the NCSs. However, to the best of the authors' knowledge, few studies have considered these factors together. In other words, the implementation of an $\mathcal{H}_\infty$ sampled-data controller with stochastic time delays and actuator faults is of practical significance.

However, there are four main challenges in this regard: First, because a mathematical analysis is difficult and complex, only a few authors have studied the stability analysis of the sampled-data NCSs. Moreover, the integral terms derived from the derivative of a LKF are more complex to handle when the stochastic time delay is considered. In addition, the conservatism is mainly related to the selection of the LKF and an over-approximation of its derivative [20]. Therefore, it is difficult to determine which method must be chosen for a reduction of the conservatism. Finally, because the actuator faults and stochastic time delay are considered, the structure of the system model becomes more complicated. The manner in which certain faultsmust be compensated for while ensuring the NCSs performance is also a difficult problem.

Thus, the present study is aimed at designing an $\mathcal{H}_\infty$ sampled-data control law, such that the NCSs with stochastic time delays and actuator faults can be asymptotically stable. By applying the Lyapunov–Krasovskii stability mechanism with an extended RCCL inequality, a novel sufficient criterion for the desired controller is provided in the form of linear matrix inequalities (LMIs). Finally, an example of a vehicle suspension as a real world applilcation is considered to prove the efficacy of the proposed method. The contributions of this paper are as follows.

(1) In contrast with [20,45], the deterministic time-varying sampling is extended to random time-varying sampling as various random external factors are considered. In addition, by considering the information of the lower bounds, the stability criterion is related to not only the upper and lower bounds of the time delay but also to the probability delay, which provides a good improvement over a reduction in the conservatism;
(2) By combining an extended RCCL method with some novel integral inequalities into the sampled-data NCSs controller design, a new sufficient condition is derived;
(3) We first consider the problem of an $\mathcal{H}_\infty$ sampled-data control approach for NCSs along with the actuator faults and probability distribution. In comparison with a related result [17], the actuator faults together with the stochastic time delays and external disturbances are further considered in this study.

The remainder of this paper is summarized as follows. The necessary problem formulation is proposed in Section 2. A novel criterion of an $\mathcal{H}_\infty$ sampled-data control approach is presented in Section 3. And, in Section 4, a numerical simulation is dis-

Table 1
Notations and descriptions.

Notations	Descriptions
$\mathbb{X}^{-1}$	The inverse matrix of $\mathbb{X}$
$\mathbb{X}^{T}$	The transposition matrix of $\mathbb{X}$
diag$\{\ldots\}$	The diagonal matrix block
$\mathbb{R}^{n}$	n-dimensional Euclidean space
$\mathbb{X} > 0$	A positive definite real symmetric matrix $\mathbb{X}$
$\mathbb{X} \geqslant 0$	A positive semi-definite real symmetric matrix $\mathbb{X}$
$\star$	$\star$ indicates symmetric elements in the symmetric matrix
$\|\cdot\|$	The Euclidean norm
$\mathcal{P}_b\{\partial\}$	The probability while event ∂ occurs
$\mathbb{E}\{\cdot\}$	Mathematical expectation
$col\{x_1 \quad \ldots \quad x_n\}$	$[x_1^T \quad \ldots \quad x_n^T]^T$
$\mathcal{L}_2[0,+\infty)$	The square-integrable vector function space over $[0,+\infty)$
$A_{n\times n}$	A $n \times n$ dimensional matrix A
$\{A\}_i$	Line i of matrix A
$sym\{A\}$	Matrix $A + A^T$

cussed to illustrate the effectiveness of the proposed design. Finally, Section 5 provides some concluding remarks. For clarity, some notations used in this paper and their corresponding descriptions are listed in Table 1.

2. Problem formulation and preliminaries

In this part, a system model is considered, which contains the control input and external disturbance

$$\begin{cases} \dot{x}(t) = Ax(t) + Bu^F(t) + Cd(t), \\ L(t) = Qx(t) + Du^F(t). \end{cases} \tag{1}$$

where $x(t) \in \mathbb{R}^n$ and $L(t) \in \mathbb{R}^l$ represent the state vector and controlled output; $u^F(t) \in \mathbb{R}^p$ is the control input; $d(t) \in \mathbb{R}^q$ indicates the external disturbance vector belonging to $\mathcal{L}_2[0,+\infty)$; and $A,\ B,\ C,\ Q$ and D are known parameter matrices with suitable dimensions.

Moreover, we define the control input with actuator faults as follows:

$$u^F(t) = Gu(t). \tag{2}$$

with

$$G = \text{diag}\{\varpi_1 \quad \varpi_2 \quad \ldots \quad \varpi_m\},\ 0 \leqslant \varpi_r \leqslant 1\ (r = 1,2,\ldots,m).$$

The matrix G represents the degree of failure of the actuator. It is clear that when $\varpi_r = 1$, the rth actuator is normal; the rth actuatorpartially malfunctions if $0 < \varpi_r < 1$; and $\varpi_r = 0$ indicates that the rth actuator has completely malfunctioned.

Remark 1. It is worth noting that the traditional state feedback control design is not applicable to a controller design owing to the control signal errors experienced in the NCSs. Thus, $u^F(t)$ is introduced to describe the control signal, which is designed to characterize such deterministic actuator faults in the system model.

Now, applying the actuator fault model (2) to (1), the system is rewritten as follows:

$$\begin{cases} \dot{x}(t) = Ax(t) + BGu(t) + Cd(t), \\ L(t) = Qx(t) + DGu(t). \end{cases} \tag{3}$$

In this study, we assume that the controller $u(t)$ is measured based on the zero-order-hold circuit and the sampling procedures prior to entrance into the networks. Moreover, t_m $(m = 0,1,\ldots)$ are the time instants that satisfy $0 \leqslant t_0 < t_1 < \cdots < t_m < \cdots$ and $\lim_{m\to\infty} t_m = \infty$. Thus, only $x(t_m)$ is usable for interval $t_m \leqslant t \leqslant t_{m+1}$. The controller $u(t)$ is then described as follows:

$$u(t) = u(t_m) = \mathcal{K}x(t_m),\ t_m \leqslant t \leqslant t_{m+1}. \tag{4}$$

where $\mathcal{K}$ represents the state-feedback gain matrix. Owing to (4), the dynamic system is expressed as follows:

$$\begin{cases} \dot{x}(t) = Ax(t) + BG\mathcal{K}x(t_m) + Cd(t), \\ L(t) = Qx(t) + DG\mathcal{K}x(t_m), \end{cases} \quad t_m \leqslant t \leqslant t_{m+1}. \tag{5}$$

Supposing that the disturbance input vector $d(t)$ belongs to $\mathcal{L}_2[0,+\infty)$, a state feedback controller gain $\mathcal{K}$ must be found that satisfies the following requirements:

(1) The system in (5) with $d(t) = 0$ is asymptotically stable;

(2) Under zero initial conditions, the $\mathcal{H}_\infty$ performance condition $\|L(t)\|_2^2 < \sigma^2\|d(t)\|_2^2$ is satisfied for any $d(t) \neq 0$, where $\|d(t)\|_2 = \sqrt{\int_{t=0}^{+\infty} |d(t)|^2 \mathrm{d}t}$ and σ is a given positive scalar.

Both continuous and discrete signals are included in the closed-loop system (5). The input delay approach is proposed to solve this problem, and thus the sampling instant t_m is defined as follows:

$$t_m = t - (t - t_m) = t - \varkappa(t).$$

We can then obtain

$$u(t) = u(t_m) = u(t - \varkappa(t)), \quad t_m \leqslant t \leqslant t_{m+1}. \tag{6}$$

where $u(t_m)$ is the discrete-time control input, and $\varkappa(t)$ is the time-varying delay.

Using the sampled-data transformation (6), the system (5) is changed into the following form:

$$\begin{cases} \dot{x}(t) = Ax(t) + BG\mathcal{K}x(t - \varkappa(t)) + Cd(t), \\ L(t) = Qx(t) + DG\mathcal{K}x(t - \varkappa(t)), \end{cases} \quad t \geqslant 0. \tag{7}$$

where $\varkappa(t)$ satisfies $\varkappa_0 \leqslant \varkappa(t) \leqslant \varkappa_2$. Here, $\varkappa_0$ and $\varkappa_2$ are constants.

Remark 2. In general, time delays often occur in a probabilistic manner owing to various external random factors or communication distractions in the NCSs. In addition, the instability, oscillation, and some other poor performance conditions are caused by probabilistic time delay signals. Therefore, adding probabilistic time delays into dynamic system models is of significant value. In this study, we consider communication signal sampling and the probability of the time delay $\varkappa(t)$ at the same time. To incorporate stochastic time delays into the system (7), the following assumptions are made.

We select two sets to describe the probability distribution of $\varkappa(t)$

$$\begin{cases} \mathbb{H}_1 = \{t | \varkappa(t) \in [\varkappa_0, \varkappa_1)\}, \\ \mathbb{H}_2 = \{t | \varkappa(t) \in [\varkappa_1, \varkappa_2]\}. \end{cases} \tag{8}$$

where apparently $\varkappa_1 \in [\varkappa_0, \varkappa_2]$, and $t \in \mathbb{H}_1$ indicates the occurence of $\varkappa(t) \in [\varkappa_0, \varkappa_1)$, and $t \in \mathbb{H}_2$ demonstrates the occurence of $\varkappa(t) \in [\varkappa_1, \varkappa_2]$. In addition, it follows from the definition (8) that $\mathbb{H}_1 \cup \mathbb{H}_2 = [0, \varkappa_2]$, $\mathbb{H}_1 \cap \mathbb{H}_2 = \varnothing$.

Remark 3. In a traditional probabilistic time delay interval division, the lower bound has usually been treated as zero [42]. A more general interval treatment that considers the information of the lower bound is proposed herein. Here, $\varkappa_0$ is chosen as the lower delay bound, the value of which does not need to be 0.

First, we assume that the probability distribution of the time-varying delay $\varkappa(t)$ satisfies $\mathcal{P}_b\{\varkappa(t) \in [\varkappa_0, \varkappa_1)\} = \xi_0$, $\mathcal{P}_b\{\varkappa(t) \in [\varkappa_1, \varkappa_2]\} = 1 - \xi_0$.

Subsequently, a Bernoulli distributed sequence $\xi(t)$ is described

$$\xi(t) = \begin{cases} 1, & \mathrm{t} \in \mathbb{H}_1, \\ 0, & \mathrm{t} \in \mathbb{H}_2. \end{cases}$$

with

$$\mathcal{P}_b\{\xi(t) = 1\} = \mathcal{P}_b\{\varkappa(t) \in [\varkappa_0, \varkappa_1)\} = \mathbb{E}\{\xi(t)\} = \xi_0.$$
$$\mathcal{P}_b\{\xi(t) = 0\} = \mathcal{P}_b\{\varkappa(t) \in [\varkappa_1, \varkappa_2]\} = 1 - \mathbb{E}\{\xi(t)\} = 1 - \xi_0.$$

Here, $\mathbb{E}\{\xi(t)\}$ is the mathematical expectation of $\xi(t)$ and $\xi_0 \in [0, 1]$ is a constant.

Furthermore, we can obtain $\mathbb{E}\{\xi(t) - \xi_0\} = 0$ and $\mathbb{E}\left\{(\xi(t) - \xi_0)^2\right\} = \xi_0(1 - \xi_0)$.

Finally, two time-varying delays $\varkappa_1(t) \in \mathbb{H}_1$ and $\varkappa_2(t) \in \mathbb{H}_2$ are introduced, and the time delays then satisfy $\varkappa_0 \leqslant \varkappa_1(t) \leqslant \varkappa_1$ and $\varkappa_1 \leqslant \varkappa_2(t) \leqslant \varkappa_2$.

Let $\varkappa_{10} = \varkappa_1 - \varkappa_0$ and $\varkappa_{21} = \varkappa_2 - \varkappa_1$. By adopting probabilistic time delays into the system model (5), we can obtain the following:

$$\begin{cases} \dot{x}(t) = Ax(t) + \xi(t)BG\mathcal{K}x(t - \varkappa_1(t)) + (1 - \xi(t))BG\mathcal{K}x(t - \varkappa_2(t)) + Cd(t), \\ \quad L(t) = Qx(t) + \xi(t)DG\mathcal{K}x(t - \varkappa_1(t) + (1 - \xi(t))DG\mathcal{K}x(t - \varkappa_2(t)). \end{cases} \tag{9}$$

This is equivalent to the following expression:

$$\begin{cases} \dot{x}(t) = & Ax(t) + \xi_0 BG\mathcal{K}x(t - \varkappa_1(t)) + (1 - \xi_0)BG\mathcal{K}x(t - \varkappa_2(t)) + Cd(t) \\ & +(\xi(t) - \xi_0)BG\mathcal{K}[x(t - \varkappa_1(t)) - x(t - \varkappa_2(t))], \\ L(t) = & Qx(t) + \xi_0 DG\mathcal{K}x(t - \varkappa_1(t)) + (1 - \xi_0)DG\mathcal{K}x(t - \varkappa_2(t)) \\ & +(\xi(t) - \xi_0)DG\mathcal{K}[x(t - \varkappa_1(t)) - x(t - \varkappa_2(t))]. \end{cases} \tag{10}$$

Before proceeding to the next section, some lemmas that are necessary to prove the main results are listed.

Lemma 1. [47]: For any symmetric matrix $S > 0$, and scalars e and f with $e < f$, let vector $x : [e,f] \in \mathbb{R}^n$ be a differentiable function; the following inequality then holds:

$$(f-e)\int_e^f \dot{x}^T(u)S\dot{x}(u)du \geqslant \sum_{i=1}^{2}(2i-1)\tau_i^T S\tau_i. \tag{11}$$

where $\tau_1 = x(f) - x(e),\ \tau_2 = x(f) + x(e) - \frac{2}{f-e}\int_e^f x(s)\mathrm{d}s$.

Lemma 2. [48]: *Let $R > 0$ be any scalar matrix with integers $e < f$, and vector $x : [e,f] \in \mathbb{R}^n$ be a differentiable function, such that the following inequality holds:*

$$-\frac{(f-e)^2}{2}\int_e^f\int_s^f x^T(u)Rx(u)\mathrm{d}u\mathrm{d}s \leqslant -\left(\int_e^f\int_s^f x(u)duds\right)^T R\left(\int_e^f\int_s^f x(u)duds\right). \tag{12}$$

Lemma 3. [30]: *For positive scalars $\beta,\ \lambda \in (0,1)$, when $\beta + \lambda = 1$, matrices $R_1,\ R_2 > 0$, and any matrices $W_1,\ W_2$, the inequality is then as follows:*

$$\begin{bmatrix} \frac{1}{\beta}R_1 & 0 \\ \star & \frac{1}{\lambda}R_2 \end{bmatrix} \geqslant \begin{bmatrix} R_1 + \lambda T_1 & \lambda W_1 + \beta W_2 \\ \star & R_2 + \beta T_2 \end{bmatrix}. \tag{13}$$

where $T_1 = R_1 - W_2R_2^{-1}W_2^T$ and $T_2 = R_2 - W_1^TR_1^{-1}W_1$.

3. Main results

In this section, the main results are discussed. The first result is given in the following theorem.

Theorem 1. *Given some scalars $\varepsilon_1, \varepsilon_2, \xi_0 > 0$ and $0 \leqslant \varkappa_0 < \varkappa_1 < \varkappa_2$, the stability of the closed-loop system (10) can be satisfied under the $\mathcal{H}_\infty$ performance index σ if there exist $3n \times 3n$ symmetric matrix $\mathcal{P} > 0, n \times n$ symmetric matrices $\mathcal{Q}_j,\ \mathcal{S}_j > 0\ (j = 1,2,3), \mathcal{R}_j > 0\ (j = 1,2,3), n \times n$ real matrix $F, 2n \times 2n$ real matrices $\vartheta_j\ (j = 1,2,3,4)$, and any matrices $\mathcal{K}$ of compatible dimensions, such that the following LMIs (14)–(21) hold*

$$\Phi_1 = \begin{bmatrix} \Upsilon_{1,[\varkappa_0,\varkappa_1]} + \Upsilon_9 - \Upsilon_2 - \Upsilon_5 - \Upsilon_6 & \mathfrak{M}_2^T\vartheta_2 & \mathfrak{M}_4^T\vartheta_4 \\ \star & -\widehat{\mathcal{R}_2} & 0 \\ \star & \star & -\widehat{\mathcal{R}_3} \end{bmatrix} < 0, \tag{14}$$

$$\Phi_2 = \begin{bmatrix} \Upsilon_{1,[\varkappa_0,\varkappa_2]} + \Upsilon_9 - \Upsilon_2 - \Upsilon_5 - \Upsilon_8 & \mathfrak{M}_2^T\vartheta_2 & \mathfrak{M}_5^T\vartheta_3^T \\ \star & -\widehat{\mathcal{R}_2} & 0 \\ \star & \star & -\widehat{\mathcal{R}_3} - \widehat{\mathcal{S}_2} \end{bmatrix} < 0, \tag{15}$$

$$\Phi_3 = \begin{bmatrix} \Upsilon_{1,[\varkappa_1,\varkappa_1]} + \Upsilon_9 - \Upsilon_2 - \Upsilon_6 - \Upsilon_7 & \mathfrak{M}_3^T\vartheta_1^T & \mathfrak{M}_4^T\vartheta_4 \\ \star & -\widehat{\mathcal{R}_2} - \widehat{\mathcal{S}_1} & 0 \\ \star & \star & -\widehat{\mathcal{R}_3} \end{bmatrix} < 0, \tag{16}$$

$$\Phi_4 = \begin{bmatrix} \Upsilon_{1,[\varkappa_1,\varkappa_2]} + \Upsilon_9 - \Upsilon_2 - \Upsilon_7 - \Upsilon_8 & \mathfrak{M}_3^T\vartheta_1^T & \mathfrak{M}_5^T\vartheta_3^T \\ \star & -\widehat{\mathcal{R}_2} - \widehat{\mathcal{S}_1} & 0 \\ \star & \star & -\widehat{\mathcal{R}_3} - \widehat{\mathcal{S}_2} \end{bmatrix} < 0, \tag{17}$$

$$\begin{bmatrix} \Upsilon_{1,[\varkappa_0,\varkappa_1]} + \Upsilon_9 - \Upsilon_2 - \Upsilon_5 - \Upsilon_6 - \Upsilon_{11} & \mathfrak{M}_2^T\vartheta_2 & \mathfrak{M}_4^T\vartheta_4 & \Upsilon_{10}^T \\ \star & -\widehat{\mathcal{R}_2} & 0 & 0 \\ \star & \star & -\widehat{\mathcal{R}_3} & 0 \\ \star & \star & \star & -I \end{bmatrix} < 0, \tag{18}$$

$$\begin{bmatrix} \Upsilon_{1,[\varkappa_0,\varkappa_2]}+\Upsilon_9-\Upsilon_2-\Upsilon_5-\Upsilon_8-\Upsilon_{11} & \mathfrak{M}_2^T\vartheta_2 & \mathfrak{M}_5^T\vartheta_3^T & \Upsilon_{10}^T \\ \star & -\widehat{\mathcal{R}_2} & 0 & 0 \\ \star & \star & -\widehat{\mathcal{R}_3}-\widehat{\mathcal{S}_2} & 0 \\ \star & \star & \star & -I \end{bmatrix} < 0, \tag{19}$$

$$\begin{bmatrix} \Upsilon_{1,[\varkappa_1,\varkappa_1]}+\Upsilon_9-\Upsilon_2-\Upsilon_6-\Upsilon_7-\Upsilon_{11} & \mathfrak{M}_3^T\vartheta_1^T & \mathfrak{M}_4^T\vartheta_4 & \Upsilon_{10}^T \\ \star & -\widehat{\mathcal{R}_2}-\widehat{\mathcal{S}_1} & 0 & 0 \\ \star & \star & -\widehat{\mathcal{R}_3} & 0 \\ \star & \star & \star & -I \end{bmatrix} < 0, \tag{20}$$

$$\begin{bmatrix} \Upsilon_{1,[\varkappa_1,\varkappa_2]}+\Upsilon_9-\Upsilon_2-\Upsilon_7-\Upsilon_8-\Upsilon_{11} & \mathfrak{M}_3^T\vartheta_1^T & \mathfrak{M}_5^T\vartheta_3^T & \Upsilon_{10}^T \\ \star & -\widehat{\mathcal{R}_2}-\widehat{\mathcal{S}_1} & 0 & 0 \\ \star & \star & -\widehat{\mathcal{R}_3}-\widehat{\mathcal{S}_2} & 0 \\ \star & \star & \star & -I \end{bmatrix} < 0. \tag{21}$$

where

$$\begin{aligned} \Upsilon_{1,[\varkappa_1(t),\varkappa_2(t)]} = \; & sym\Big\{\Gamma_1^T\mathcal{P}\Gamma_2\Big\}+\mathfrak{m}_2^T\mathcal{Q}_1\mathfrak{m}_2-\mathfrak{m}_4^T(\mathcal{Q}_1-\mathcal{Q}_2)\mathfrak{m}_4-\mathfrak{m}_6^T\mathcal{Q}_2\mathfrak{m}_6 \\ & +\mathfrak{m}_{13}^T\big[\varkappa_{10}^2\mathcal{R}_2+\varkappa_{21}^2\mathcal{R}_3+\tfrac{1}{2}\varkappa_{10}^2\mathcal{S}_1+\tfrac{1}{2}\varkappa_{21}^2\mathcal{S}_2\big]\mathfrak{m}_{13}, \end{aligned}$$

$$\Upsilon_2 = \; 2\mathfrak{M}_6^T\mathcal{S}_1\mathfrak{M}_6+2\mathfrak{M}_7^T\mathcal{S}_1\mathfrak{M}_7+2\mathfrak{M}_8^T\mathcal{S}_2\mathfrak{M}_8+2\mathfrak{M}_9^T\mathcal{S}_2\mathfrak{M}_9,$$

$$\Upsilon_5 = \; \begin{bmatrix}\mathfrak{M}_2\\ \mathfrak{M}_3\end{bmatrix}^T\begin{bmatrix}2\widehat{\mathcal{R}_2}+\widehat{\mathcal{S}_1} & \vartheta_1\\ \star & \widehat{\mathcal{R}_2}\end{bmatrix}\begin{bmatrix}\mathfrak{M}_2\\ \mathfrak{M}_3\end{bmatrix},$$

$$\Upsilon_6 = \; \begin{bmatrix}\mathfrak{M}_4\\ \mathfrak{M}_5\end{bmatrix}^T\begin{bmatrix}2\widehat{\mathcal{R}_3}+\widehat{\mathcal{S}_2} & \vartheta_3\\ \star & \widehat{\mathcal{R}_3}\end{bmatrix}\begin{bmatrix}\mathfrak{M}_4\\ \mathfrak{M}_5\end{bmatrix},$$

$$\Upsilon_7 = \; \begin{bmatrix}\mathfrak{M}_2\\ \mathfrak{M}_3\end{bmatrix}^T\begin{bmatrix}\widehat{\mathcal{R}_2} & \vartheta_2\\ \star & 2\widehat{\mathcal{R}_2}\end{bmatrix}\begin{bmatrix}\mathfrak{M}_2\\ \mathfrak{M}_3\end{bmatrix},$$

$$\Upsilon_8 = \; \begin{bmatrix}\mathfrak{M}_4\\ \mathfrak{M}_5\end{bmatrix}^T\begin{bmatrix}\widehat{\mathcal{R}_3} & \vartheta_4\\ \star & 2\widehat{\mathcal{R}_3}\end{bmatrix}\begin{bmatrix}\mathfrak{M}_4\\ \mathfrak{M}_5\end{bmatrix},$$

$$\Upsilon_9 = \; (\varepsilon_1\mathfrak{m}_1^TF+\varepsilon_2\mathfrak{m}_{13}^TF)\psi,$$

$$\Upsilon_{10} = \; Q\mathfrak{m}_1+\xi_0DG\mathcal{K}\mathfrak{m}_3+(1-\xi_0)DG\mathcal{K}\mathfrak{m}_5,$$

$$\Upsilon_{11} = \; \sigma^2\mathfrak{m}_{12}^T\mathfrak{m}_{12},$$

$$\psi = \; \Big[A \quad 0 \quad \xi_0BG\mathcal{K} \quad 0 \quad (1-\xi_0)BG\mathcal{K} \quad \underbrace{0\ldots0}_{7\times} \quad C \quad -I\Big],$$

$$\Gamma_1 = \; \mathrm{col}\{\mathfrak{m}_1 \quad (\varkappa_1(t)-\varkappa_0)\mathfrak{m}_8+(\varkappa_1-\varkappa_1(t))\mathfrak{m}_9 \quad (\varkappa_2(t)-\varkappa_1)\mathfrak{m}_{10}+(\varkappa_2-\varkappa_2(t))\mathfrak{m}_{11}\},$$

$$\Gamma_2 = \mathrm{col}\{\,\mathfrak{m}_{13} \quad \mathfrak{m}_2-\mathfrak{m}_4 \quad \mathfrak{m}_4-\mathfrak{m}_6\,\},$$

$$\mathfrak{m}_j = \big[\,0_{n\times(j-1)n} \quad I_{n\times n} \quad 0_{n\times(12-j)n+1}\,\big], \quad j=1,2,\ldots,11,$$

$$\mathfrak{m}_{12} = [\,0_{1\times11n} \quad I_{1\times1} \quad 0_{1\times n}\,],$$

$$\mathfrak{m}_{13} = [\,0_{n\times11n+1} \quad I_{n\times n}\,],$$

$$\mathfrak{M}_j = \mathrm{col}\{\ \mathfrak{m}_j - \mathfrak{m}_{j+1} \quad \mathfrak{m}_j + \mathfrak{m}_{j+1} - 2\mathfrak{m}_{j+6}\ \},\quad j = 1,2,\ldots,5,$$

$$\mathfrak{M}_6 = \mathfrak{m}_2 - \mathfrak{m}_8,\quad \mathfrak{M}_7 = \mathfrak{m}_3 - \mathfrak{m}_9,\quad \mathfrak{M}_8 = \mathfrak{m}_4 - \mathfrak{m}_{10},\quad \mathfrak{M}_9 = \mathfrak{m}_5 - \mathfrak{m}_{11},$$

$$\widehat{\mathcal{R}_1} = \begin{bmatrix} \mathcal{R}_1 & 0 \\ 0 & 3\mathcal{R}_1 \end{bmatrix},\quad \widehat{\mathcal{R}_2} = \begin{bmatrix} \mathcal{R}_2 & 0 \\ 0 & 3\mathcal{R}_2 \end{bmatrix},\quad \widehat{\mathcal{R}_3} = \begin{bmatrix} \mathcal{R}_3 & 0 \\ 0 & 3\mathcal{R}_3 \end{bmatrix},$$
$$\widehat{\mathcal{S}_1} = \begin{bmatrix} \mathcal{S}_1 & 0 \\ 0 & 3\mathcal{S}_1 \end{bmatrix},\quad \widehat{\mathcal{S}_2} = \begin{bmatrix} \mathcal{S}_2 & 0 \\ 0 & 3\mathcal{S}_2 \end{bmatrix}.$$

Proof. The following Lyapunov–Krasovskii functional is constructed for the closed-loop system (10)

$$V(x(t)) = V_1(x(t)) + V_2(x(t)) + V_3(x(t)) + V_4(x(t)). \tag{22}$$

where

$$V_1(x(t)) = \rho^T(t)\mathcal{P}\rho(t), \tag{23}$$

$$V_2(x(t)) = \int_{t-\varkappa_1}^{t-\varkappa_0} x^T(u)\mathcal{Q}_1 x(u)\mathrm{d}u + \int_{t-\varkappa_2}^{t-\varkappa_1} x^T(u)\mathcal{Q}_2 x(u)\mathrm{d}u, \tag{24}$$

$$\begin{aligned} V_3(x(t)) = {} & \varkappa_0 \int_{-\varkappa_0}^{0}\int_{t+s}^{t} \dot{x}^T(u)\mathcal{R}_1\dot{x}(u)\mathrm{d}u\mathrm{d}s + \varkappa_{10}\int_{-\varkappa_1}^{-\varkappa_0}\int_{t+s}^{t}\dot{x}^T(u)\mathcal{R}_2\dot{x}(u)\mathrm{d}u\mathrm{d}s \\ & + \varkappa_{21}\int_{-\varkappa_2}^{-\varkappa_1}\int_{t+s}^{t}\dot{x}^T(u)\mathcal{R}_3\dot{x}(u)\mathrm{d}u\mathrm{d}s, \end{aligned} \tag{25}$$

$$V_4(x(t)) = \int_{-\varkappa_1}^{-\varkappa_0}\int_{\theta}^{-\varkappa_0}\int_{t+s}^{t}\dot{x}^T(u)\mathcal{S}_1\dot{x}(u)\mathrm{d}u\mathrm{d}s\mathrm{d}\theta + \int_{-\varkappa_2}^{-\varkappa_1}\int_{\theta}^{-\varkappa_1}\int_{t+s}^{t}\dot{x}^T(u)\mathcal{S}_2\dot{x}(u)\mathrm{d}u\mathrm{d}s\mathrm{d}\theta. \tag{26}$$

with $\rho(t) = col\Big\{x(t) \quad \int_{t-\varkappa_1}^{t-\varkappa_0} x(u)\mathrm{d}u \quad \int_{t-\varkappa_2}^{t-\varkappa_1} x(u)\mathrm{d}u\Big\}$.

Then, taking the time derivative of $V(x(t))$, we have

$$\dot{V}_1(x(t)) = sym\{\rho^T(t)\mathcal{P}\dot{\rho}(t)\}, \tag{27}$$

$$\begin{aligned} \dot{V}_2(x(t)) = {} & x^T(t-\varkappa_0)\mathcal{Q}_1 x(t-\varkappa_0) - x^T(t-\varkappa_1)(\mathcal{Q}_1-\mathcal{Q}_2)x(t-\varkappa_1) \\ & - x^T(t-\varkappa_2)\mathcal{Q}_2 x(t-\varkappa_2), \end{aligned} \tag{28}$$

$$\dot{V}_3(x(t)) = \dot{x}^T(t)\big[\varkappa_0^2\mathcal{R}_1 + \varkappa_{10}^2\mathcal{R}_2 + \varkappa_{21}^2\mathcal{R}_3\big]\dot{x}(t) + \alpha_1(t) + \alpha_2(t) + \alpha_3(t). \tag{29}$$

where

$$\begin{aligned} \alpha_1(t) = {} & -\varkappa_0\int_{t-\varkappa_0}^{t}\dot{x}^T(u)\mathcal{R}_1\dot{x}(u)\mathrm{d}u, \\ \alpha_2(t) = {} & -\varkappa_{10}\int_{t-\varkappa_1}^{t-\varkappa_0}\dot{x}^T(u)\mathcal{R}_2\dot{x}(u)\mathrm{d}u, \\ \alpha_3(t) = {} & -\varkappa_{21}\int_{t-\varkappa_2}^{t-\varkappa_1}\dot{x}^T(u)\mathcal{R}_3\dot{x}(u)\mathrm{d}u. \end{aligned}$$

By applying Lemma 1 to estimate the single integral terms $\alpha_1(t), \alpha_2(t)$, and $\alpha_3(t)$, we obtain

$$\begin{aligned} \alpha_1(t) \leqslant {} & -\begin{bmatrix}\eta_1\\ \eta_2\end{bmatrix}^T\begin{bmatrix}\mathcal{R}_1 & 0\\ \star & 3\mathcal{R}_1\end{bmatrix}\begin{bmatrix}\eta_1\\ \eta_2\end{bmatrix}, \\ \alpha_2(t) \leqslant {} & -\tfrac{\varkappa_{10}}{\varkappa_1-\varkappa_1(t)}\begin{bmatrix}\eta_3\\ \eta_4\end{bmatrix}^T\begin{bmatrix}\mathcal{R}_2 & 0\\ \star & 3\mathcal{R}_2\end{bmatrix}\begin{bmatrix}\eta_3\\ \eta_4\end{bmatrix} \\ & -\tfrac{\varkappa_{10}}{\varkappa_1(t)-\varkappa_0}\begin{bmatrix}\eta_5\\ \eta_6\end{bmatrix}^T\begin{bmatrix}\mathcal{R}_2 & 0\\ \star & 3\mathcal{R}_2\end{bmatrix}\begin{bmatrix}\eta_5\\ \eta_6\end{bmatrix}, \\ \alpha_3(t) \leqslant {} & -\tfrac{\varkappa_{21}}{\varkappa_2-\varkappa_2(t)}\begin{bmatrix}\eta_7\\ \eta_8\end{bmatrix}^T\begin{bmatrix}\mathcal{R}_3 & 0\\ \star & 3\mathcal{R}_3\end{bmatrix}\begin{bmatrix}\eta_7\\ \eta_8\end{bmatrix} \\ & -\tfrac{\varkappa_{21}}{\varkappa_2(t)-\varkappa_1}\begin{bmatrix}\eta_9\\ \eta_{10}\end{bmatrix}^T\begin{bmatrix}\mathcal{R}_3 & 0\\ \star & 3\mathcal{R}_3\end{bmatrix}\begin{bmatrix}\eta_9\\ \eta_{10}\end{bmatrix}. \end{aligned} \tag{30}$$

where

$$\begin{aligned}
\eta_1 &= x(t)-x(t-\varkappa_0), \quad \eta_2 = x(t)+x(t-\varkappa_0)-2\int_{t-\varkappa_0}^{t}\frac{x(u)}{\varkappa_0}\mathrm{d}u,\\
\eta_3 &= x(t-\varkappa_1(t))-x(t-\varkappa_1), \quad \eta_4 = x(t-\varkappa_1(t))+x(t-\varkappa_1)-2\int_{t-\varkappa_1}^{t-\varkappa_1(t)}\frac{x(u)}{\varkappa_1-\varkappa_1(t)}\mathrm{d}u,\\
\eta_5 &= x(t-\varkappa_0)-x(t-\varkappa_1(t)), \quad \eta_6 = x(t-\varkappa_0)+x(t-\varkappa_1(t))-2\int_{t-\varkappa_1(t)}^{t-\varkappa_0}\frac{x(u)}{\varkappa_1(t)-\varkappa_0}\mathrm{d}u,\\
\eta_7 &= x(t-\varkappa_2(t))-x(t-\varkappa_2), \quad \eta_8 = x(t-\varkappa_2(t))+x(t-\varkappa_2)-2\int_{t-\varkappa_2}^{t-\varkappa_2(t)}\frac{x(u)}{\varkappa_2-\varkappa_2(t)}\mathrm{d}u,\\
\eta_9 &= x(t-\varkappa_1)-x(t-\varkappa_2(t)), \quad \eta_{10} = x(t-\varkappa_1)+x(t-\varkappa_2(t))-2\int_{t-\varkappa_2(t)}^{t-\varkappa_1}\frac{x(u)}{\varkappa_2(t)-\varkappa_1}\mathrm{d}u.
\end{aligned}$$

In addition, the derivative of $V_4(x(t))$ is obtained as follows:

$$\dot{V}_4(x(t)) = \dot{x}^T(t)\left[\frac{1}{2}\varkappa_{10}^2\mathcal{S}_1+\frac{1}{2}\varkappa_{21}^2\mathcal{S}_2\right]\dot{x}(t)+\alpha_4(t)+\alpha_5(t)+\alpha_6(t)+\alpha_7(t)+\alpha_8(t)+\alpha_9(t). \tag{31}$$

where

$$\alpha_4(t) = -\int_{-\varkappa_1(t)}^{-\varkappa_0}\int_{t+s}^{t-\varkappa_0}\dot{x}^T(u)\mathcal{S}_1\dot{x}(u)\mathrm{d}u\mathrm{d}s,$$

$$\alpha_5(t) = -(\varkappa_1-\varkappa_1(t))\int_{t-\varkappa_1(t)}^{t-\varkappa_0}\dot{x}^T(u)\mathcal{S}_1\dot{x}(u)\mathrm{d}u\mathrm{d}s,$$

$$\alpha_6(t) = -\int_{-\varkappa_1}^{-\varkappa_1(t)}\int_{t+s}^{t-\varkappa_1(t)}\dot{x}^T(u)\mathcal{S}_1\dot{x}(u)\mathrm{d}u\mathrm{d}s,$$

$$\alpha_7(t) = -\int_{-\varkappa_2(t)}^{-\varkappa_1}\int_{t+s}^{t-\varkappa_1}\dot{x}^T(u)\mathcal{S}_2\dot{x}(u)\mathrm{d}u\mathrm{d}s,$$

$$\alpha_8(t) = -(\varkappa_2-\varkappa_2(t))\int_{t-\varkappa_2(t)}^{t-\varkappa_1}\dot{x}^T(u)\mathcal{S}_2\dot{x}(u)\mathrm{d}u\mathrm{d}s,$$

$$\alpha_9(t) = -\int_{-\varkappa_2}^{-\varkappa_2(t)}\int_{t+s}^{t-\varkappa_2(t)}\dot{x}^T(u)\mathcal{S}_2\dot{x}(u)\mathrm{d}u\mathrm{d}s.$$

By using Lemma 1, new upper bounds are found for the single integral terms $\alpha_5(t)$ and $\alpha_8(t)$:

$$\begin{aligned}
\alpha_5(t) \leqslant\ & -\frac{\varkappa_{10}}{\varkappa_1(t)-\varkappa_0}\begin{bmatrix}\eta_{10}\\ \eta_{11}\end{bmatrix}^T\begin{bmatrix}\mathcal{S}_1 & 0\\ \star & 3\mathcal{S}_1\end{bmatrix}\begin{bmatrix}\eta_{10}\\ \eta_{11}\end{bmatrix}\\
& +\begin{bmatrix}\eta_{10}\\ \eta_{11}\end{bmatrix}^T\begin{bmatrix}\mathcal{S}_1 & 0\\ \star & 3\mathcal{S}_1\end{bmatrix}\begin{bmatrix}\eta_{10}\\ \eta_{11}\end{bmatrix},\\
\alpha_8(t) \leqslant\ & -\frac{\varkappa_{21}}{\varkappa_2(t)-\varkappa_1}\begin{bmatrix}\eta_{12}\\ \eta_{13}\end{bmatrix}^T\begin{bmatrix}\mathcal{S}_2 & 0\\ \star & 3\mathcal{S}_2\end{bmatrix}\begin{bmatrix}\eta_{12}\\ \eta_{13}\end{bmatrix}\\
& +\begin{bmatrix}\eta_{12}\\ \eta_{13}\end{bmatrix}^T\begin{bmatrix}\mathcal{S}_2 & 0\\ \star & 3\mathcal{S}_2\end{bmatrix}\begin{bmatrix}\eta_{12}\\ \eta_{13}\end{bmatrix}.
\end{aligned} \tag{32}$$

where

$$\begin{aligned}
\eta_{10} &= x(t-\varkappa_0)-x(t-\varkappa_1(t)),\\
\eta_{11} &= x(t-\varkappa_0)+x(t-\varkappa_1(t))-2\int_{t-\varkappa_1(t)}^{t-\varkappa_0}\frac{x(u)}{\varkappa_1(t)-\varkappa_0}\mathrm{d}u,\\
\eta_{12} &= x(t-\varkappa_1)-x(t-\varkappa_2(t)),\\
\eta_{13} &= x(t-\varkappa_1)+x(t-\varkappa_2(t))-2\int_{t-\varkappa_2(t)}^{t-\varkappa_1}\frac{x(u)}{\varkappa_2(t)-\varkappa_1}\mathrm{d}u.
\end{aligned}$$

Then, using Lemma 2 on the double integral terms $\alpha_4(t)$, $\alpha_6(t)$, $\alpha_7(t)$, and $\alpha_9(t)$, we get

$$\begin{aligned}
\alpha_4(t)+\alpha_6(t)+\alpha_7(t)+\alpha_9(t) \leqslant\ & -2\begin{bmatrix}\eta_{14}\\ \eta_{15}\end{bmatrix}^T\begin{bmatrix}\mathcal{S}_1 & 0\\ \star & \mathcal{S}_1\end{bmatrix}\begin{bmatrix}\eta_{14}\\ \eta_{15}\end{bmatrix}\\
& -2\begin{bmatrix}\eta_{16}\\ \eta_{17}\end{bmatrix}^T\begin{bmatrix}\mathcal{S}_2 & 0\\ \star & \mathcal{S}_2\end{bmatrix}\begin{bmatrix}\eta_{16}\\ \eta_{17}\end{bmatrix}.
\end{aligned} \tag{33}$$

where

$$\eta_{14} = x(t-\varkappa_0) - \int_{t-\varkappa_1(t)}^{t-\varkappa_0} \frac{x(u)}{\varkappa_1(t)-\varkappa_0}\mathrm{d}u,$$

$$\eta_{15} = x(t-\varkappa_1(t)) - \int_{t-\varkappa_1}^{t-\varkappa_1(t)} \frac{x(u)}{\varkappa_1-\varkappa_1(t)}\mathrm{d}u,$$

$$\eta_{16} = x(t-\varkappa_1) - \int_{t-\varkappa_2(t)}^{t-\varkappa_1} \frac{x(u)}{\varkappa_2(t)-\varkappa_1}\mathrm{d}u,$$

$$\eta_{17} = x(t-\varkappa_2(t)) - \int_{t-\varkappa_2}^{t-\varkappa_2(t)} \frac{x(u)}{\varkappa_2-\varkappa_2(t)}\mathrm{d}u.$$

For further simplification, the following definitions are given:

$$\begin{aligned}\Upsilon_{1,[\varkappa_1(t),\varkappa_2(t)]} = \; & sym\Big\{\Gamma_1^T\mathcal{P}\Gamma_2\Big\} + \mathfrak{m}_2^T\mathcal{Q}_1\mathfrak{m}_2 - \mathfrak{m}_4^T(\mathcal{Q}_1-\mathcal{Q}_2)\mathfrak{m}_4 - \mathfrak{m}_6^T\mathcal{Q}_2\mathfrak{m}_6 \\ & +\mathfrak{m}_{13}^T\big[\varkappa_{10}^2\mathcal{R}_2 + \varkappa_{21}^2\mathcal{R}_3 + \tfrac{1}{2}\varkappa_{10}^2\mathcal{S}_1 + \tfrac{1}{2}\varkappa_{21}^2\mathcal{S}_2\big]\mathfrak{m}_{13},\end{aligned}$$

and

$$\Upsilon_2 = 2\mathfrak{M}_6^T\mathcal{S}_1\mathfrak{M}_6 + 2\mathfrak{M}_7^T\mathcal{S}_1\mathfrak{M}_7 + 2\mathfrak{M}_8^T\mathcal{S}_2\mathfrak{M}_8 + 2\mathfrak{M}_9^T\mathcal{S}_2\mathfrak{M}_9.$$

We then take the mathematical expectation of $\dot{V}(x(t))$, which can be written as:

$$\begin{aligned}\mathbb{E}\Big\{\dot{V}(x(t))\Big\} \; \leqslant \; & \gamma^T(t)\Big[\Upsilon_{1,[\varkappa_1(t),\varkappa_2(t)]} - \Upsilon_2 + \mathfrak{M}_2^T\widehat{\mathcal{S}_1}\mathfrak{M}_2 + \mathfrak{M}_4^T\widehat{\mathcal{S}_2}\mathfrak{M}_4\Big]\gamma(t) \\ & -\gamma^T(t)\left[\frac{\varkappa_{10}\mathfrak{M}_2^T\left(\widehat{\mathcal{S}_1}+\widehat{\mathcal{R}_2}\right)\mathfrak{M}_2}{\varkappa_1(t)-\varkappa_0} + \frac{\varkappa_{10}\mathfrak{M}_3^T\widehat{\mathcal{R}_2}\mathfrak{M}_3}{\varkappa_1-\varkappa_1(t)}\right]\gamma(t) \\ & -\gamma^T(t)\left[\frac{\varkappa_{21}\mathfrak{M}_4^T\left(\widehat{\mathcal{S}_2}+\widehat{\mathcal{R}_3}\right)\mathfrak{M}_4}{\varkappa_2(t)-\varkappa_1} + \frac{\varkappa_{21}\mathfrak{M}_5^T\widehat{\mathcal{R}_3}\mathfrak{M}_5}{\varkappa_2-\varkappa_2(t)}\right]\gamma(t).\end{aligned} \tag{34}$$

where

$$\begin{aligned}\gamma(t) = \; & col\{x(t) \quad x(t-\varkappa_0) \quad x(t-\varkappa_1(t)) \quad x(t-\varkappa_1) \quad x(t-\varkappa_2(t)) \quad x(t-\varkappa_2) \\ & \textstyle\int_{t-\varkappa_0}^{t}\frac{x(u)}{\varkappa_0}\mathrm{d}u \quad \int_{t-\varkappa_1(t)}^{t-\varkappa_0}\frac{x(u)}{\varkappa_1(t)-\varkappa_0}\mathrm{d}u \quad \int_{t-\varkappa_1}^{t-\varkappa_1(t)}\frac{x(u)}{\varkappa_1-\varkappa_1(t)}\mathrm{d}u \\ & \textstyle\int_{t-\varkappa_2(t)}^{t-\varkappa_1}\frac{x(u)}{\varkappa_2(t)-\varkappa_1}\mathrm{d}u \quad \int_{t-\varkappa_2}^{t-\varkappa_2(t)}\frac{x(u)}{\varkappa_2-\varkappa_2(t)}\mathrm{d}u \quad d(t) \quad \dot{x}(t)\Big\}.\end{aligned}$$

By utilizing Lemma 3, it follows that

$$\begin{aligned}&\gamma(t)^T\left[\frac{\varkappa_{10}\mathfrak{M}_2^T\left(\widehat{\mathcal{S}_1}+\widehat{\mathcal{R}_2}\right)\mathfrak{M}_2}{\varkappa_1(t)-\varkappa_0} + \frac{\varkappa_{10}\mathfrak{M}_3^T\widehat{\mathcal{R}_2}\mathfrak{M}_3}{\varkappa_1-\varkappa_1(t)} - \mathfrak{M}_2^T\widehat{\mathcal{S}_1}\mathfrak{M}_2\right]\gamma(t) \geqslant \gamma(t)^T\Upsilon_{3,[\varkappa_1(t)]}\gamma(t), \\ &\gamma(t)^T\left[\frac{\varkappa_{21}\mathfrak{M}_4^T\left(\widehat{\mathcal{S}_2}+\widehat{\mathcal{R}_3}\right)\mathfrak{M}_4}{\varkappa_2(t)-\varkappa_1} + \frac{\varkappa_{21}\mathfrak{M}_5^T\widehat{\mathcal{R}_3}\mathfrak{M}_5}{\varkappa_2-\varkappa_2(t)} - \mathfrak{M}_4^T\widehat{\mathcal{S}_2}\mathfrak{M}_4\right]\gamma(t) \geqslant \gamma(t)^T\Upsilon_{4,[\varkappa_2(t)]}\gamma(t).\end{aligned} \tag{35}$$

where

$$\begin{aligned}\Upsilon_{3,[\varkappa_1(t)]} \; = \; & \mathfrak{M}_2^T\left(\widehat{\mathcal{R}_2}+\widehat{\mathcal{S}_1}\right)\mathfrak{M}_2 + \mathfrak{M}_3^T\widehat{\mathcal{R}_2}\mathfrak{M}_3 - \mathfrak{M}_2^T\widehat{\mathcal{S}_1}\mathfrak{M}_2 \\ & + \frac{\varkappa_1-\varkappa_1(t)}{\varkappa_{10}}\begin{bmatrix}\mathfrak{M}_2\\ \mathfrak{M}_3\end{bmatrix}^T\begin{bmatrix}\widehat{\mathcal{R}_2}+\widehat{\mathcal{S}_1}-\vartheta_2\widehat{\mathcal{R}_2}^{-1}\vartheta_2^T & \vartheta_1\\ \star & 0\end{bmatrix}\begin{bmatrix}\mathfrak{M}_2\\ \mathfrak{M}_3\end{bmatrix} \\ & + \frac{\varkappa_1(t)-\varkappa_0}{\varkappa_{10}}\begin{bmatrix}\mathfrak{M}_2\\ \mathfrak{M}_3\end{bmatrix}^T\begin{bmatrix}0 & \vartheta_2\\ \star & \widehat{\mathcal{R}_2}-\vartheta_1^T\left(\widehat{\mathcal{R}_2}+\widehat{\mathcal{S}_1}\right)^{-1}\vartheta_1\end{bmatrix}\begin{bmatrix}\mathfrak{M}_2\\ \mathfrak{M}_3\end{bmatrix}.\end{aligned} \tag{36}$$

and

$$\begin{aligned}\Upsilon_{4,[\varkappa_2(t)]} \; = \; & \mathfrak{M}_4^T\left(\widehat{\mathcal{R}_3}+\widehat{\mathcal{S}_2}\right)\mathfrak{M}_4 + \mathfrak{M}_5^T\widehat{\mathcal{R}_3}\mathfrak{M}_5 - \mathfrak{M}_4^T\widehat{\mathcal{S}_2}\mathfrak{M}_4 \\ & + \frac{\varkappa_2-\varkappa_2(t)}{\varkappa_{21}}\begin{bmatrix}\mathfrak{M}_4\\ \mathfrak{M}_5\end{bmatrix}^T\begin{bmatrix}\widehat{\mathcal{R}_3}+\widehat{\mathcal{S}_2}-\vartheta_4\widehat{\mathcal{R}_3}^{-1}\vartheta_4^T & \vartheta_3\\ \star & 0\end{bmatrix}\begin{bmatrix}\mathfrak{M}_4\\ \mathfrak{M}_5\end{bmatrix} \\ & + \frac{\varkappa_2(t)-\varkappa_1}{\varkappa_{21}}\begin{bmatrix}\mathfrak{M}_4\\ \mathfrak{M}_5\end{bmatrix}^T\begin{bmatrix}0 & \vartheta_4\\ \star & \widehat{\mathcal{R}_3}-\vartheta_3^T\left(\widehat{\mathcal{R}_3}+\widehat{\mathcal{S}_2}\right)^{-1}\vartheta_3\end{bmatrix}\begin{bmatrix}\mathfrak{M}_4\\ \mathfrak{M}_5\end{bmatrix}.\end{aligned} \tag{37}$$

Therefore, the mathematical expectation of $\dot{V}(x(t))$ can be estimated as:

$$\mathbb{E}\left\{\dot{V}(x(t))\right\} \leqslant \gamma^T(t)\left[\Upsilon_{1,[\varkappa_1(t),\varkappa_2(t)]} - \Upsilon_2 - \Upsilon_{3,[\varkappa_1(t)]} - \Upsilon_{4,[\varkappa_2(t)]}\right]\gamma(t). \tag{38}$$

In addition, for any matrix F with the appropriate dimensions, we obtain the following:

$$\begin{aligned}&\mathbb{E}\{sym\{\left[\varepsilon_1 x^T(t)F + \varepsilon_2 \dot{x}^T(t)F\right][-\dot{x}(t) + Ax(t) + \xi_0 BG\mathcal{K}x(t-\varkappa_1(t)) + (1-\xi_0)BG\mathcal{K}x(t-\varkappa_2(t))\\ &+Cd(t) + (\xi(t)-\xi_0)BG\mathcal{K}[x(t-\varkappa_1(t)) - x(t-\varkappa_2(t))]]\}\}\\ &= sym\{\left[\varepsilon_1 x^T(t)F + \varepsilon_2 \dot{x}^T(t)F\right][-\dot{x}(t) + Ax(t) + \xi_0 BG\mathcal{K}x(t-\varkappa_1(t)) + (1-\xi_0)BG\mathcal{K}x(t-\varkappa_2(t)) + Cd(t)]\} = 0.\end{aligned} \tag{39}$$

Then, by adding Eq. (39), which uses a slack matrix method, into $\dot{V}(x(t))$, the equation is rewritten as:

$$\mathbb{E}\left\{\dot{V}(x(t))\right\} \leqslant \gamma^T(t)\left[\Upsilon_{1,[\varkappa_1(t),\varkappa_2(t)]} + \Upsilon_9 - \Upsilon_2 - \Upsilon_{3,[\varkappa_1(t)]} - \Upsilon_{4,[\varkappa_2(t)]}\right]\gamma(t). \tag{40}$$

where

$$\Upsilon_9 = sym\{\Lambda_1\psi\},\ \Lambda_1 = col\left\{\varepsilon_1 F \quad \underbrace{0\ldots0}_{11\times} \quad 0_{n\times1} \quad \varepsilon_2 F\right\},$$

$$\psi = \left[A \quad 0 \quad \xi_0 BG\mathcal{K} \quad 0 \quad (1-\xi_0)BG\mathcal{K} \quad \underbrace{0\ldots0}_{7\times} \quad C \quad -I\right].$$

It is evident that $\Upsilon_{1,[\varkappa_1(t),\varkappa_2(t)]} - \Upsilon_2 - \Upsilon_{3,[\varkappa_1(t)]} - \Upsilon_{4,[\varkappa_2(t)]} + \Upsilon_9 < 0$ holds only if the following four conditions based on the convex combination theorem are satisfied:

$$\Upsilon_{1,[\varkappa_0,\varkappa_1]} + \Upsilon_9 - \Upsilon_2 - \Upsilon_{3,[\varkappa_0]} - \Upsilon_{4,[\varkappa_1]} < 0, \tag{41}$$

$$\Upsilon_{1,[\varkappa_0,\varkappa_2]} + \Upsilon_9 - \Upsilon_2 - \Upsilon_{3,[\varkappa_0]} - \Upsilon_{4,[\varkappa_2]} < 0, \tag{42}$$

$$\Upsilon_{1,[\varkappa_1,\varkappa_1]} + \Upsilon_9 - \Upsilon_2 - \Upsilon_{3,[\varkappa_1]} - \Upsilon_{4,[\varkappa_1]} < 0, \tag{43}$$

$$\Upsilon_{1,[\varkappa_1,\varkappa_2]} + \Upsilon_9 - \Upsilon_2 - \Upsilon_{3,[\varkappa_1]} - \Upsilon_{4,[\varkappa_2]} < 0. \tag{44}$$

which are guaranteed by matrix inequalities (14)–(17) through the Schur complement.

Therefore, $\mathbb{E}\left\{\dot{V}(x(t))\right\} < 0$ is satisfied such that the asymptotic stability of the system (10) is established. Next, considering the $\mathcal{H}_\infty$ performance of the closed-loop system, we have

$$\begin{aligned}&\mathbb{E}\left\{\dot{V}(x(t))\right\} + \mathbb{E}\left\{L^T(t)L(t) - \sigma^2 d^T(t)d(t)\right\}\\ &= \gamma^T(t)\left[\Upsilon_{1,[\varkappa_1(t),\varkappa_2(t)]} + \Upsilon_9 - \Upsilon_2 - \Upsilon_{3,[\varkappa_1(t)]} - \Upsilon_{4,[\varkappa_2(t)]} + \Upsilon_{10}^T\Upsilon_{10} - \Upsilon_{11}\right]\gamma(t).\end{aligned} \tag{45}$$

where $\Upsilon_{10} = Q\mathfrak{m}_1 + \xi_0 DG\mathcal{K}\mathfrak{m}_3 + (1-\xi_0)DG\mathcal{K}\mathfrak{m}_5$ and $\Upsilon_{11} = \sigma^2\mathfrak{m}_{12}^T\mathfrak{m}_{12}$.

By applying the Schur complement, matrix inequalities (18)–(21) guarantee the following:

$$\gamma^T(t)\left[\Upsilon_{1,[\varkappa_1(t),\varkappa_2(t)]} + \Upsilon_9 + \Upsilon_{10}^T\Upsilon_{10} - \Upsilon_2 - \Upsilon_{3,[\varkappa_1(t)]} - \Upsilon_{4,[\varkappa_2(t)]} - \Upsilon_{11}\right]\gamma(t) < 0. \tag{46}$$

Therefore, from (46) we get $\mathbb{E}\left\{\dot{V}(x(t))\right\} + \mathbb{E}\left\{L^T(t)L(t) - \sigma^2 d^T(t)d(t)\right\} < 0$.

For any $d(t) \neq 0$, it implies that $V(0) = 0$ and $V(+\infty) \geqslant 0$ under zero initial conditions. Integrating the inequality $\mathbb{E}\left\{\dot{V}(x(t))\right\} + \mathbb{E}\left\{L^T(t)L(t) - \sigma^2 d^T(t)d(t)\right\} < 0$, we have

$$\int_0^{+\infty} \mathbb{E}\left\{L^T(t)L(t)\right\}dt - \int_0^{+\infty} \mathbb{E}\left\{\sigma^2 d^T(t)d(t)\right\}dt < \mathbb{E}\{V(0)\} - \mathbb{E}\{V(+\infty)\} < 0. \tag{47}$$

which means the $\mathcal{H}_\infty$ performance condition $\|L(t)\|^2 < \sigma^2\|d(t)\|^2$ is achieved. Also, this implies that the system (10) is guaranteed to be stable. Therefore, the proof is completed. ■

It can be seen that the controller gain $\mathcal{K}$ is related to the matrix F. Thus, Theorem 1 cannot be solved directly using the LMIs toolbox. The method for calculating the gain $\mathcal{K}$ is as follows.

Remark 4. In this study, the Bessel-Legendre inequality [47] is used to handle single-integral terms. And Lemma 2 [48] is applied to over-approximate double-integral terms. These two aforementioned inequalities have been proved to be an effective approach to decreasing the conservatism. By combining an extended reciprocally convex matrix lemma with these integral inequalities to establish the stability of the NCSs, a large upper bound of the time-varying delay is obtained, and thus the proposed method can further reduce the conservatism.

Theorem 2. *For some given positive scalars $\varepsilon_1, \varepsilon_2, \xi_0$ and $0 \leqslant \varkappa_0 < \varkappa_1 < \varkappa_2$, the stability of the closed-loop system (10) can be satisfied under the $\mathcal{H}_\infty$ performance index σ if there exist symmetric $3n \times 3n$ matrix $\mathcal{P} > 0, n \times n$ symmetric matrices $\mathcal{Q}_j,\ \mathcal{S}_j > 0\ (j = 1,2), \mathcal{R}_j > 0\ (j = 1,2,3), n \times n$ real matrix F, and $2n \times 2n$ real matrices $\vartheta_j\ (j = 1,2,3,4)$, as well as any matrices $\mathcal{K}$ of compatible dimensions, such that the following LMIs hold:*

$$\begin{bmatrix} \Xi_{1,[\varkappa_0,\varkappa_1]} - \overline{\Upsilon}_5 - \overline{\Upsilon}_6 & \mathfrak{M}_2^T\overline{\vartheta}_2 & \mathfrak{M}_4^T\overline{\vartheta}_4 & \overline{\Upsilon}_{10}^T \\ \star & -\overline{\widehat{\mathcal{R}_2}} & 0 & 0 \\ \star & \star & -\overline{\widehat{\mathcal{R}_3}} & 0 \\ \star & \star & \star & -I \end{bmatrix} < 0, \tag{48}$$

$$\begin{bmatrix} \Xi_{1,[\varkappa_0,\varkappa_2]} - \overline{\Upsilon}_5 - \overline{\Upsilon}_8 & \mathfrak{M}_2^T\overline{\vartheta}_2 & \mathfrak{M}_5^T\overline{\vartheta}_3^T & \overline{\Upsilon}_{10}^T \\ \star & -\overline{\widehat{\mathcal{R}_2}} & 0 & 0 \\ \star & \star & -\overline{\widehat{\mathcal{R}_3}} - \overline{\widehat{\mathcal{S}_2}} & 0 \\ \star & \star & \star & -I \end{bmatrix} < 0, \tag{49}$$

$$\begin{bmatrix} \Xi_{1,[\varkappa_1,\varkappa_1]} - \overline{\Upsilon}_6 - \overline{\Upsilon}_7 & \mathfrak{M}_3^T\overline{\vartheta}_1^T & \mathfrak{M}_4^T\overline{\vartheta}_4 & \overline{\Upsilon}_{10}^T \\ \star & -\overline{\widehat{\mathcal{R}_2}} - \overline{\widehat{\mathcal{S}_1}} & 0 & 0 \\ \star & \star & -\overline{\widehat{\mathcal{R}_3}} & 0 \\ \star & \star & \star & -I \end{bmatrix} < 0, \tag{50}$$

$$\begin{bmatrix} \Xi_{1,[\varkappa_1,\varkappa_2]} - \overline{\Upsilon}_7 - \overline{\Upsilon}_8 & \mathfrak{M}_3^T\overline{\vartheta}_1^T & \mathfrak{M}_5^T\overline{\vartheta}_3^T & \overline{\Upsilon}_{10}^T \\ \star & -\overline{\widehat{\mathcal{R}_2}} - \overline{\widehat{\mathcal{S}_1}} & 0 & 0 \\ \star & \star & -\overline{\widehat{\mathcal{R}_3}} - \overline{\widehat{\mathcal{S}_2}} & 0 \\ \star & \star & \star & -I \end{bmatrix} < 0, \tag{51}$$

$$\begin{aligned} \Xi_{1,[\varkappa_1(t),\varkappa_2(t)]} &= sym\left\{\Gamma_1^T\overline{\mathcal{P}}\Gamma_2\right\} + \mathfrak{m}_2^T\overline{\mathcal{Q}}_1\mathfrak{m}_2 - \mathfrak{m}_4^T(\overline{\mathcal{Q}}_1 - \overline{\mathcal{Q}}_2)\mathfrak{m}_4 - \mathfrak{m}_6^T\overline{\mathcal{Q}}_2\mathfrak{m}_6 \\ &+\mathfrak{m}_{13}^T\left[(\varkappa_1 - \varkappa_0)^2\overline{\mathcal{R}}_2 + (\varkappa_2 - \varkappa_1)^2\overline{\mathcal{R}}_3 + \tfrac{1}{2}\varkappa_{10}^2\overline{\mathcal{S}}_1 + \tfrac{1}{2}\varkappa_{21}^2\overline{\mathcal{S}}_2\right]\mathfrak{m}_{13} \\ &+sym\left\{\overline{\Lambda}_1\overline{\psi}\right\} - \mathfrak{m}_{12}^T\sigma^2 I\mathfrak{m}_{12} - 2\mathfrak{M}_6^T\overline{\mathcal{S}}_1\mathfrak{M}_6 - 2\mathfrak{M}_7^T\overline{\mathcal{S}}_1\mathfrak{M}_7 - 2\mathfrak{M}_8^T\overline{\mathcal{S}}_2\mathfrak{M}_8 - 2\mathfrak{M}_9^T\overline{\mathcal{S}}_2\mathfrak{M}_9, \end{aligned}$$

$$\overline{\Upsilon}_5 = \begin{bmatrix}\mathfrak{M}_2 \\ \mathfrak{M}_3\end{bmatrix}^T\begin{bmatrix} 2\overline{\widehat{\mathcal{R}_2}} + \overline{\widehat{\mathcal{S}_1}} & \overline{\vartheta}_1 \\ \star & \overline{\widehat{\mathcal{R}_2}}\end{bmatrix}\begin{bmatrix}\mathfrak{M}_2 \\ \mathfrak{M}_3\end{bmatrix},$$

$$\overline{\Upsilon}_6 = \begin{bmatrix}\mathfrak{M}_4 \\ \mathfrak{M}_5\end{bmatrix}^T\begin{bmatrix} 2\overline{\widehat{\mathcal{R}_3}} + \overline{\widehat{\mathcal{S}_2}} & \overline{\vartheta}_3 \\ \star & \overline{\widehat{\mathcal{R}_3}}\end{bmatrix}\begin{bmatrix}\mathfrak{M}_4 \\ \mathfrak{M}_5\end{bmatrix},$$

$$\overline{\Upsilon}_7 = \begin{bmatrix}\mathfrak{M}_2 \\ \mathfrak{M}_3\end{bmatrix}^T\begin{bmatrix} \overline{\widehat{\mathcal{R}_2}} & \overline{\vartheta}_2 \\ \star & 2\overline{\widehat{\mathcal{R}_2}}\end{bmatrix}\begin{bmatrix}\mathfrak{M}_2 \\ \mathfrak{M}_3\end{bmatrix},$$

$$\overline{\Upsilon}_8 = \begin{bmatrix}\mathfrak{M}_4 \\ \mathfrak{M}_5\end{bmatrix}^T\begin{bmatrix} \overline{\widehat{\mathcal{R}_3}} & \overline{\vartheta}_4 \\ \star & 2\overline{\widehat{\mathcal{R}_3}}\end{bmatrix}\begin{bmatrix}\mathfrak{M}_4 \\ \mathfrak{M}_5\end{bmatrix},$$

$$\overline{\Upsilon}_{10} = \overline{\mathcal{Q}}\mathfrak{m}_1 + \xi_0 DGN\mathfrak{m}_3 + (1 - \xi_0)DGN\mathfrak{m}_5,$$

$$\overline{\Lambda_1} = col\left\{\varepsilon_1 I \quad \underbrace{0\ldots0}_{10\times} \quad 0_{n\times 1} \quad \varepsilon_2 I\right\},$$

$$\overline{\psi} = \left[A\overline{F} \quad 0 \quad \xi_0 BGN \quad 0 \quad (1-\xi_0)BGN \quad \underbrace{0\ldots0}_{6\times} \quad C \quad -\overline{F}\right],$$

$$\widehat{\overline{\mathcal{R}_1}} = \begin{bmatrix} \overline{\mathcal{R}}_1 & 0 \\ 0 & 3\overline{\mathcal{R}}_1 \end{bmatrix}, \quad \widehat{\overline{\mathcal{R}_2}} = \begin{bmatrix} \overline{\mathcal{R}}_2 & 0 \\ 0 & 3\overline{\mathcal{R}}_2 \end{bmatrix}, \quad \widehat{\overline{\mathcal{R}_3}} = \begin{bmatrix} \overline{\mathcal{R}}_3 & 0 \\ 0 & 3\overline{\mathcal{R}}_3 \end{bmatrix},$$

$$\widehat{\overline{\mathcal{S}_2}} = \begin{bmatrix} \overline{\mathcal{S}}_2 & 0 \\ 0 & 3\overline{\mathcal{S}}_2 \end{bmatrix}, \quad \widehat{\overline{\mathcal{S}_3}} = \begin{bmatrix} \overline{\mathcal{S}}_3 & 0 \\ 0 & 3\overline{\mathcal{S}}_3 \end{bmatrix}.$$

The feedback control matrix $\mathcal{K}$ is then described as follows:

$$\mathcal{K} = N\overline{F}^{-1}. \tag{52}$$

Proof. Set

$$\overline{F} = F^{-1},\ \widetilde{F}_1 = diag\{\overline{F} \quad \overline{F}\},\ \widetilde{F}_2 = diag\{\overline{F} \quad \overline{F} \quad \overline{F}\},\ \overline{\mathcal{P}} = \widetilde{F}_2^T \mathcal{P} \widetilde{F}_2,\ \overline{\mathcal{Q}}_i = \overline{F}^T \mathcal{Q}_i \overline{F}\ (i = 1,2),$$

$$\overline{\mathcal{R}}_i = \overline{F}^T \mathcal{R}_i \overline{F}\ (i = 1,2,3),\ \overline{\mathcal{S}}_i = \overline{F}^T \mathcal{S}_i \overline{F}\ (i = 1,2),\ N = \mathcal{K}\overline{F},\ \overline{\vartheta}_i = \widetilde{F}_1^T \vartheta_i \widetilde{F}_1\ (i = 1,2,3,4),$$

$$J_1 = diag\left\{\underbrace{\overline{F}\ldots\overline{F}}_{11\times} \quad I_{n\times 1} \quad \overline{F}\right\},\ J_2 = diag\left\{J_1 \quad \widetilde{F}_1 \quad \widetilde{F}_1 \quad I_{n-1\times n-1}\right\}.$$

Multiplying both sides of (18)–(21) by J_2^T and J_2, we obtain (48)–(51). And the controller gain $\mathcal{K}$ is given by (52). Thus, the proof has been completed. ■

Remark 5. When the stochastic time delays and failure mechanisms are not considered, the research problem is reduced to that described in [17,49]. In this case, a better $\mathcal{H}_\infty$ performance can be obtained when compared with the results derived in [17,49] due to the structure of $V(x(t))$, and the method for an estimation the upper bound of the integral terms. Owing to the length restriction, the theorem is omitted herein. In addition, the comparison results are given in the following numerical simulation part.

4. Numerical simulation

In this section, a numerical example is used to prove the efficiency of the proposed control method. For the simulation requirements, a vehicle suspension model with two degrees of freedom is taken into account [17], as shown in Fig. 1.

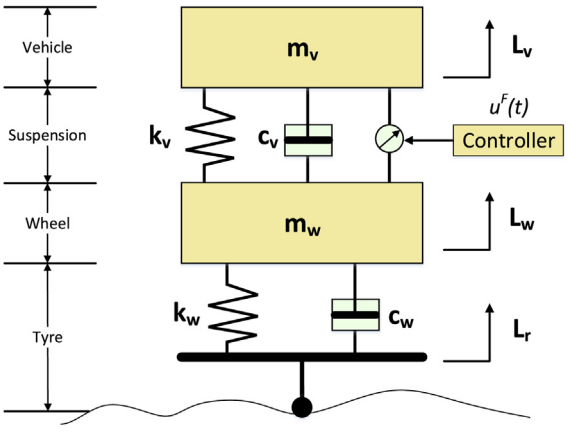

Fig. 1. Quarter-vehicle system with an active suspension.

And the dynamic equations are formulated based on [13], which consider the performance requirements of vehicle ride comfort, firm uninterrupted contact of the wheels on the road, reasonable suspension deflection, and limited power of the actuator.

$$\begin{cases} m_v\ddot{L}_v(t) + c_v\left[\dot{L}_v(t) - \dot{L}_w(t)\right] + k_v[L_v(t) - L_w(t)] = u(t), \\ m_w\ddot{L}_w(t) + c_v\left[\dot{L}_w(t) - \dot{L}_v(t)\right] + k_v[L_w(t) - L_v(t)] + k_w[L_w(t) - L_r(t)] + c_w\left[\dot{L}_w(t) - \dot{L}_r(t)\right] = -u(t), \\ L_1(t) = \ddot{L}_v(t), \\ L_2(t) = \left[\frac{L_v(t)-L_w(t)}{L_{\max}} \quad \frac{k_w(L_w(t)-L_r(t))}{(m_v+m_w)g}\right]^T. \end{cases} \tag{53}$$

where the sprung mass denoting the chassis of the vehicle is described as m_v; the unsprung mass denoting the mass of the wheel assembly is indicated by m_w; $u(t)$ is the active control of the system; the damping coefficient and compressibility of a pneumatic tyre are described by k_w and c_w, respectively; the damping coefficient and stiffness of the system are expressed through k_v and c_v, respectively; the vertical displacements of the sprung and unsprung masses are depicted by $L_v(t)$ and $L_w(t)$, respectively; and the road displacement input is indicated by $L_r(t)$.

Remark 6. A vehicle suspension is a typical networked control system. And the vehicle suspension has been widely studied as an important aspect of the vehicle chassis performance [7,12,13,17,48], so that it has been proved to be an effective model for the simulation of the controller design.

For the previous proposed active suspension system model, we define the following:

$$\begin{cases} x_1(t) = L_v(t) - L_w(t),\ x_2(t) = L_w(t) - L_r(t),\ x_3(t) = \dot{L}_v(t),\ x_4(t) = \dot{L}_w(t), \\ x(t) = [x_1(t) \quad x_2(t) \quad x_3(t) \quad x_4(t)]^T. \end{cases} \tag{54}$$

where state variables $x_1(t)$ represents the suspension deflection; $x_2(t)$ indicates the tyre deflection; $x_3(t)$ and $x_4(t)$ indicate the speed of the sprung and unsprung massed, respectively; and $d(t)$ represents the disturbance input.

Then, we obtain the state-space form of the suspension system

$$\begin{cases} \dot{x}(t) &= Ax(t) + Bu(t) + Cd(t), \\ L_1(t) &= Q_1x(t) + D_1u(t), \\ L_2(t) &= Q_2x(t). \end{cases} \tag{55}$$

where

$$A = \begin{bmatrix} 0 & 0 & 1 & -1 \\ 0 & 0 & 0 & 1 \\ -\frac{k_v}{m_v} & 0 & -\frac{c_v}{m_v} & \frac{c_v}{m_v} \\ \frac{k_v}{m_w} & -\frac{k_w}{m_w} & \frac{c_v}{m_w} & -\frac{c_v+c_w}{m_w} \end{bmatrix}, \quad B = \begin{bmatrix} 0 \\ 0 \\ \frac{1}{m_v} \\ -\frac{1}{m_w} \end{bmatrix}, \quad C = \begin{bmatrix} 0 \\ -1 \\ 0 \\ \frac{c_w}{m_w} \end{bmatrix}, \quad d(t) = \dot{L}_r,$$

$$Q_1 = \begin{bmatrix} -\frac{k_v}{m_v} & 0 & -\frac{c_v}{m_v} & \frac{c_v}{m_v} \end{bmatrix}, \quad D_1 = \frac{1}{m_v}, \quad Q_2 = \begin{bmatrix} \frac{1}{L_{max}} & 0 & 0 & 0 \\ 0 & \frac{k_w}{(m_v+m_w)g} & 0 & 0 \end{bmatrix}.$$

Let

$$L(t) = \begin{bmatrix} L_1(t) \\ L_2(t) \end{bmatrix} = Qx(t) + Du(t). \tag{56}$$

in which

$$Q = \begin{bmatrix} Q_1 \\ Q_2 \end{bmatrix}, \quad D = \begin{bmatrix} D_1 \\ 0 \end{bmatrix}.$$

The system model parameters utilized in the subsequent simulation are listed in Table 2, which were selected from the results presented in [13].

By taking the $\mathcal{H}_\infty$ sampled-data control law, the actuator faults, and the stochastic time delays into account, the above dynamic Eqs. (55) and (56) are formulated as follows:

$$\begin{cases} \dot{x}(t) = & Ax(t) + \xi_0 BG\mathcal{K}x(t - \varkappa_1(t)) + (1 - \xi_0)BG\mathcal{K}x(t - \varkappa_2(t)) + Cd(t) \\ & +(\xi(t) - \xi_0)BG\mathcal{K}[x(t - \varkappa_1(t)) - x(t - \varkappa_2(t))], \\ L(t) = & Qx(t) + \xi_0 DG\mathcal{K}x(t - \varkappa_1(t)) + (1 - \xi_0)DG\mathcal{K}x(t - \varkappa_2(t)) \\ & +(\xi(t) - \xi_0)DG\mathcal{K}[x(t - \varkappa_1(t)) - x(t - \varkappa_2(t))]. \end{cases}$$

Table 2
Parameters of quarter-car active suspension system.

Parameter	m_v	m_w	k_v	k_w	c_v	c_w
Value	320 kg	40 kg	18 kN/m	200 kN/m	1 kN s/m	10 N s/m

where

$$A=\begin{bmatrix} 0 & 0 & 1 & -1 \\ 0 & 0 & 0 & 1 \\ -56.25 & 0 & -3.125 & 3.125 \\ 450 & -5000 & 25 & -25.25 \end{bmatrix},\quad B=\begin{bmatrix} 0 \\ 0 \\ 0.0031 \\ -0.025 \end{bmatrix},\quad C=\begin{bmatrix} 0 \\ -1 \\ 0 \\ 0.25 \end{bmatrix},$$

$$Q=\begin{bmatrix} -56.25 & 0 & -3.125 & 3.125 \\ 10 & 0 & 0 & 0 \\ 0 & 56.6893 & 0 & 0 \end{bmatrix},\quad D=\begin{bmatrix} 0.0031 \\ 0 \\ 0 \end{bmatrix}.$$

To prove the effectiveness of the designed controller, we consider several response requirements: the active force $u(t)$, the suspension deflection $x_1(t)$, the tyre deflection $x_2(t)$, and the controlled and performance outputs which can be gained from $L(t)$.

The active force $u(t)$ should be constrained below the limited power u_{max}. In addition, the vertical body acceleration $L_1(t)$ should be sufficiently small, and the suspension deflection must be less than the maximum reasonable suspension deflection L_{max}. And the firm uninterrupted contact of the wheels with road $k_w[L_w(t)-L_r(t)]<(m_v+m_w)g$, described in $L(t)$, should be satisfied.

First, the actuator faults are assumed to occur in the vehicle suspension system model, and the actuator faults rate is chosen as $G=0.5$. We then assume that the maximum reasonable suspension deflection L_{max} and the maximum force output u_{max} are set as 0.1 m and 1500 N, respectively. Moreover, the additional parameters are selected as $\varepsilon_1=1,\ \varepsilon_2=0.2$. For the given $\xi_0=0.1$ and $\varkappa_0=0.01$ s, $\varkappa_1=0.02$ s, $\varkappa_2=0.04$ s, the minimum allowable values of σ for different values of $\varkappa_2$ are shown in Table 3, which indicates that the $\mathcal{H}_\infty$ performance index increases as the upper bound $\varkappa_2$ decreases.

To evaluate the simulation results, we consider two types of road conditions in this study: bump and the limited ramp road conditions. For the first condition, road disturbances can generally be assumed as shocks, caused by obvious bumps or pits on a flat road. In this study, this type of bumpy road disturbance signal along with Power Spectral Density vibration [48] is utilized to evaluate the controller design approach, which is given by the following:

$$d(t)=\begin{cases} \frac{h\pi v}{l}\sin\left(\frac{2\pi v}{l}t\right), & \text{if} \quad 0\leqslant t\leqslant l/v \\ 0, & \text{if} \quad t>l/v \end{cases} \tag{57}$$

where h indicates the height of the bumps, and l represents the length of the bumpy road. In addition, the forward car speed is represented by v.

Assume that $h=0.06$ m, $l=5$ m and $v=36$ km/h. By employing the convex optimization algorithm, the minimum guaranteed $\mathcal{H}_\infty$ performance index is estimated as $\sigma=11.7782$. And the admissible control gain matrix $\mathcal{K}$ is computed as follows:

$$\mathcal{K}=10^4\times[3.2362\quad 3.2166\quad 0.0370\quad 0.0281]. \tag{58}$$

Using the admissible control gain matrix $\mathcal{K}$, the variation $\xi(t)$ of the Bernoulli probability distribution is displayed in Fig. 2. The responses of the suspension deflection, tyre deflection, active force, and vertical body acceleration on the bumpy road are shown in Fig. 3, respectively. And the controlled output constraints are plotted in Fig. 4, where $\{L_2(t)\}_1$ and $\{L_2(t)\}_2$ are composed in the solid and dashed lines. Under the condition of an actuator failure, it is evident that the requirements of the design are properly satisfied based on these simulation results.

The suspension deflection $x_1(t)$ is below the maximum reasonable suspension deflection $L_{max}=0.1$ m. The limitation of the control signal $|u_{max}|=1500$ N is satisfied by the active force $u^F(t)$. It can be seen from Fig. 3 that the vehicle body acceleration and the tire deflection achieve a good outcome. In addition, the constrained output conditions $|L_2(t)|<1$ are guaranteed, as shown in Fig. 4. Moreover, the maximum allowable upper bounds (MAUB) of $\varkappa_2$ for different values of $\varkappa_1$ are depicted in Table 4, and it is evident that for a larger bound of $\varkappa_2$, $\varkappa_1$ is larger.

Table 3
Minimum allowable values of σ for different values of $\varkappa_2$ ($\varkappa_1=0.02s, \xi_0=0.1$).

$\varkappa_2$	0.5 s	0.1 s	0.08 s	0.06 s	0.04 s
σ	21.7857	12.5769	12.2105	11.9538	11.7782

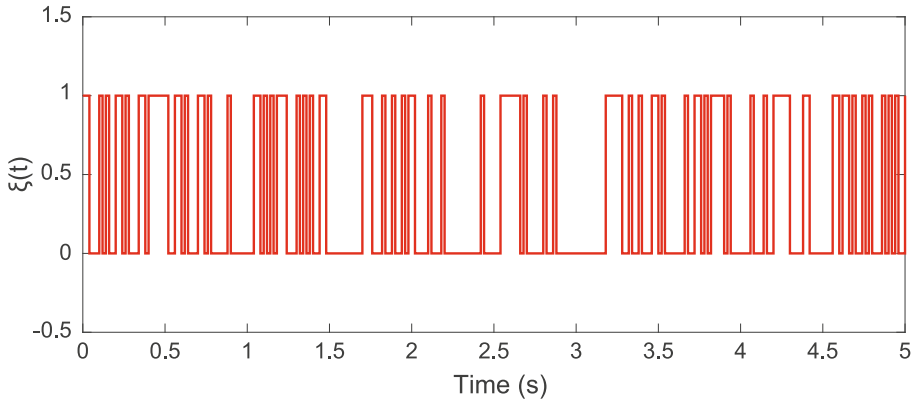

Fig. 2. Bernoulli random variable $\xi(t)$.

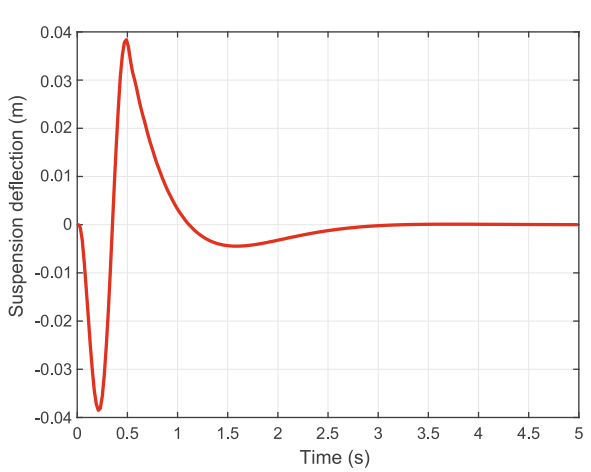

(a) Suspension deflection

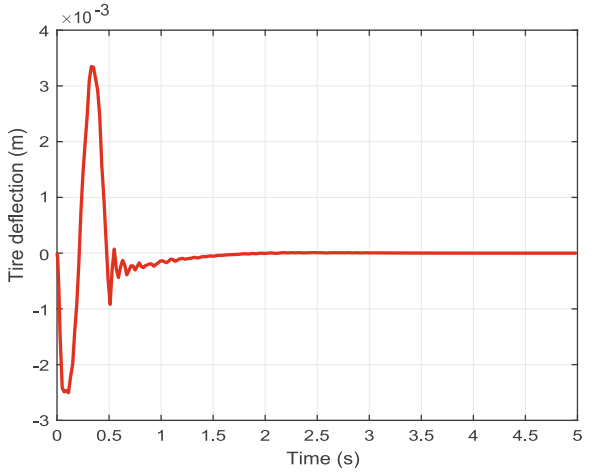

(b) Tire deflection

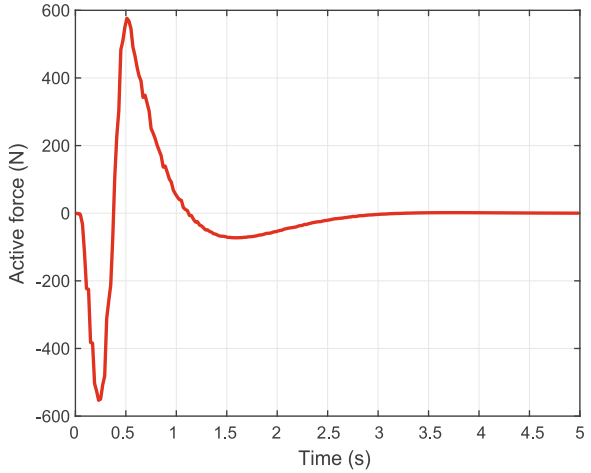

(c) Active force

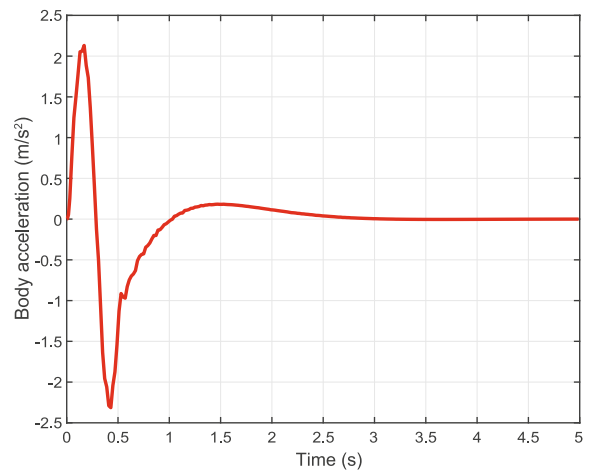

(d) Body acceleration

Fig. 3. Performance responses for suspension system on bumpy road.

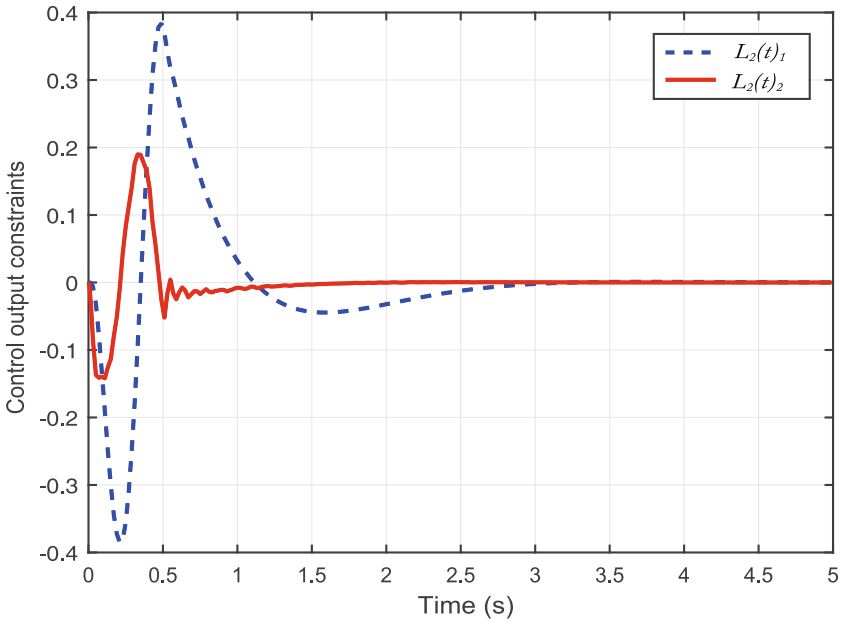

Fig. 4. The controlled output constraints on bumpy road $\{L_2(t)\}_i$ $(i = 1, 2)$.

Table 4
MAUB of $\varkappa_2$ for different values of $\varkappa_1$ $(\xi_0 = 0.1, \sigma = 20)$.

$\varkappa_1$	0.02 s	0.04 s	0.06 s	0.08 s	0.1 s
$\varkappa_2$	0.21 s	0.22 s	0.24 s	0.25 s	0.26 s

Second, a type of limited ramp load condition is taken into account. This road condition can test the effectiveness of the proposed controller when the elevation of road surface changes. The change in road elevation can be described as:

$$L_r(t) = \begin{cases} 0, & \text{if} \quad 0 \leqslant t \leqslant 1 \\ 5H(t-1), & \text{if} \quad 1 < t \leqslant 1.2 \\ H, & \text{if} \quad t > 1.2 \end{cases}$$

where H is the final height of the road ramp.

And the disturbance input $d(t)$ represents the velocity of the road roughness, that is, $d(t) = \dot{L}_r(t)$. In this simulation part, we choose $H = 0.2$m. Moreover, the related performance responses for the suspension system on a limited ramp road are shown in Figs. 5 and 6.

The responses of the suspension deflection, tyre deflection, active force, and vertical body acceleration on a limited ramp road are shown in Fig. 5. And the controlled output constraints are plotted in Fig. 6. It can be seen from these figures that tall constrained are within an allowable range. In addition, the output constraint conditions $|L_2(t)| < 1$ are guaranteed.

Next, we show that the controller design with probabilistic time delays gains less conservative results. By comparison, the lower bound is assumed as a constant $\varkappa_0 = 0.01$ s. We then suppose the guaranteed $\mathcal{H}_\infty$ performance index is $\sigma = 20$. If only the sampling period is considered, the allowable sampling period is 0.18 s. However, we obtain a larger maximum sampling period if we consider probabilistic time delays, that is, there are multiple sampling periods. For instance, assuming that $\varkappa_1 = 0.02$ s and $\xi_0 = 0.5$, the allowable maximum upper bound of $\varkappa_2$ is 0.33 s, which reveals that taking the probabilistic time delays into consideration makes the controller less conservative. Table 6 shows that, when ξ_0 increases, the minimum allowable $\mathcal{H}_\infty$ performance index is smaller. Additionally, more detailed comparison results are shown in Tables 5 and 6.

It is concluded from the simulation results that good performances are achieved for the vehicle suspension model under the condition of the actuator failure. The $\mathcal{H}_\infty$ performance and hard constraints are satisfied with the proposed controller. Therefore, the proposed method is valid for the NCSs along with stochastic time delays and actuator faults.

For a comparison with the existing sampled-data $\mathcal{H}_\infty$ methods for a suspension model [17,49], we consider theorems with no actuator faults and stochastic time delays in this study. Furthermore, the lower bounders of the time delays are set to 0. Using the vehicle model parameters in [17,49], we obtain the minimum allowable σ for different MAUB of the time delays shown in Table 7. Results from previous studies [17,49] are also shown in Table 7 for comparison purpose. It can be found that the results of the current study are less conservative than those of [17,49]. Moreover, none of the abovementioned stud-

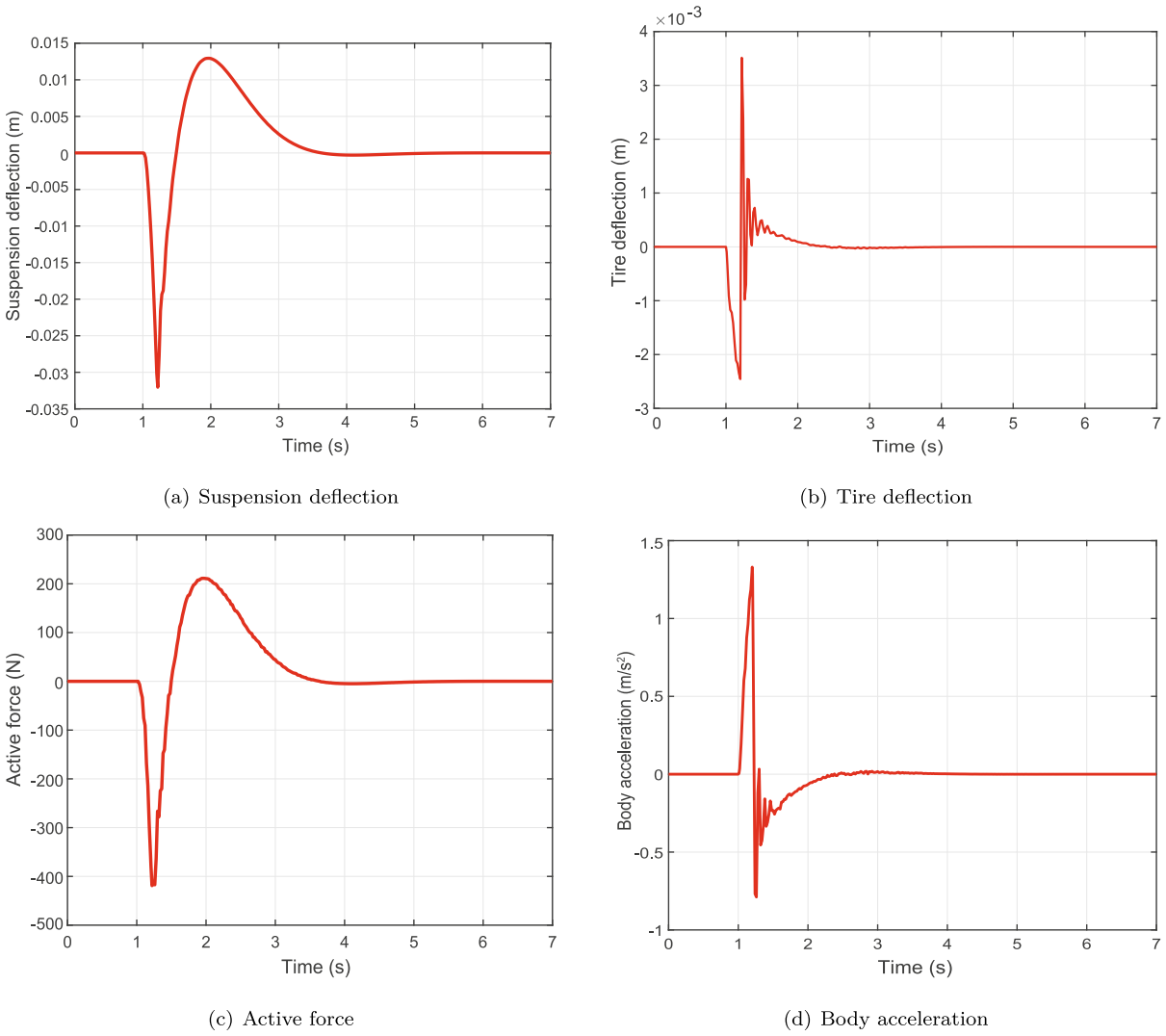

(a) Suspension deflection (b) Tire deflection

(c) Active force (d) Body acceleration

Fig. 5. Performance responses for suspension system on limited ramp load.

ies on suspension systems have solved the problem of actuator faults and stochastic delays. Therefore, the method developed in this study is more general and effective.

5. Conclusion

In this study, the problem of fault-tolerant $\mathcal{H}_\infty$ sampled-data control for the NCSs was investigated, including probability delay signals and actuator faults. By introducing the input delay approach and Bernoulli distribution, the $\mathcal{H}_\infty$ sampled-data control system was changed into a system together with probabilistic time delays. Furthermore, by utilizing the extended reciprocally convex matrix inequality, we obtained a novel delay-dependent stability criterion. Finally, a quarter-vehicle suspension system was taken into account to illustrate the benefit and effectiveness of the proposed control approach. Note that many practical NCSs may be sensitive to specific frequency bands. Hence, it is meaningful to consider the finite frequency $\mathcal{H}_\infty$ control method in a future study, which can further improve the effectiveness and application range of the proposed method. Additionally, another possible research avenue is the further reduction of the conservatism through an improved LKF. Moreover, an event-triggered sampling scheme can save communication resources via reducing the number of samplings [48]. Therefore, an event-triggered control scheme for NCSs will be focused on in the future.

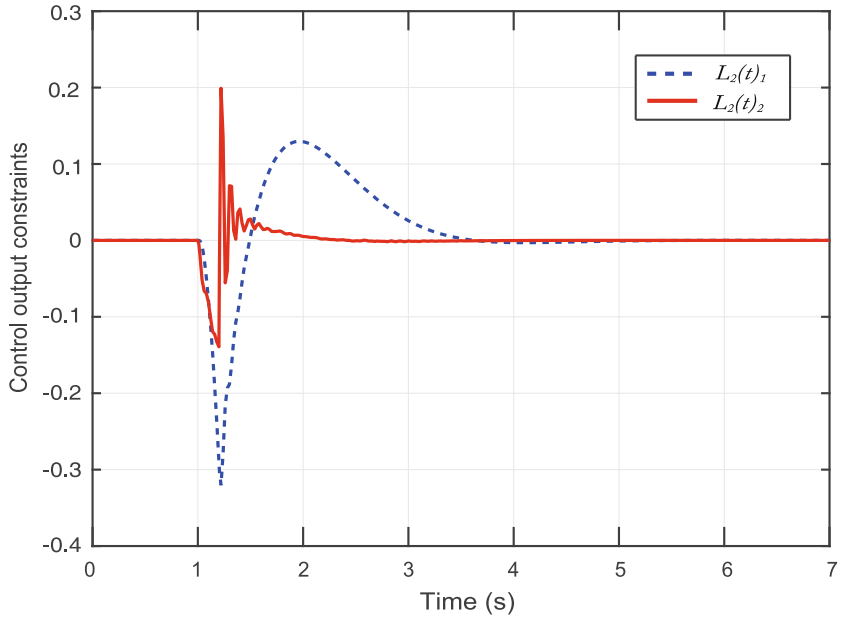

Fig. 6. The controlled output constraints on limited ramp load $\{L_2(t)\}_i$ $(i = 1, 2)$.

Table 6
Minimum allowable values of σ for different values of ξ_0 ($\varkappa_1 = 0.02$ s, $\varkappa_2 = 0.04$ s).

ξ_0	0.9	0.7	0.5	0.3	0.1
σ	11.7073	11.7169	11.7312	11.7494	11.7782

Table 5
MAUB of $\varkappa_2$ for different values of ξ_0 ($\varkappa_1 = 0.02$ s, $\sigma = 20$).

ξ_0	0.9	0.7	0.5	0.3	0.1
$\varkappa_2$	2.95 s	0.63 s	0.33 s	0.25 s	0.21 s

Table 7
Minimum allowable values of σ for different MAUB of $\varkappa$.

$\varkappa$	0.005 s	0.010 s	0.015 s	0.020 s	0.025 s
[17]	8.3651	8.6758	9.7879	12.4934	21.6790
[49]	9.8577	10.2824	11.1341	12.6120	19.8366
Remark 6	6.5112	6.8179	7.3127	7.6643	7.9525

CRediT authorship contribution statement

Fang Fang: Conceptualization, Project administration, Software, Writing - original draft. **Haotian Ding:** Writing - original draft, Methodology. **Yajuan Liu:** Writing - review & editing, Data curation, Supervision. **Ju H. Park:** Validation, Visualization, Writing - review & editing, Supervision.

Declaration of Competing Interest

The authors declare that they have no known competing financial interests or personal relationships that could have appeared to influence the work reported in this paper.

Acknowledgment

The work of Fang Fang, Haotian Ding, and Yajuan Liu was supported by the National Science and Technology Major Project of China under Grant 2017-V-0010-0061, and the National Science Foundation of China under Grant (61803153,

51676068). Also, the work of J.H. Park was supported by the National Research Foundation of Korea (NRF) grant funded by the Korea government (Ministry of Science and ICT) (No. 2019R1A5A808029011).

References

[1] B. Tang, J. Wang, Y. Zhang, A delay-distribution approach to stabilization of networked control systems, IEEE Trans. Control Network Syst. 2 (2015) 382–392.
[2] T.C. Yang, Networked control system: a brief survey, IEE Proc. Control Theory Appl. 153 (2006) 403–412.
[3] Y.-L. Wang, T.-B. Wang, Q.-L. Han, Fault detection filter design for data reconstruction-based continuous-time networked control systems, Inf. Sci. 328 (2016) 577–594.
[4] K. Wang, E. Tian, J. Liu, L. Wei, D. Yue, Resilient control of networked control systems under deception attacks: a memory-event-triggered communication scheme, Int. J. Robust Nonlinear Control 30 (2020) 1534–1548.
[5] C. Li, H. Jing, R. Wang, N. Chen, Vehicle lateral motion regulation under unreliable communication links based on robust $\mathcal{H}_\infty$ output-feedback control schema, Mech. Syst. Signal Process. 104 (2018) 171–187.
[6] H. Hu, M. Zhou, Z. Li, Y. Tang, An optimization approach to improved petri net controller design for automated manufacturing systems, IEEE Trans. Autom. Sci. Eng. 10 (2013) 772–782.
[7] C. Hong, G. Kong-Hui, Constrained $\mathcal{H}_\infty$ control of active suspensions: an LMI approach, IEEE Trans. Control Syst. Technol. 13 (2005) 412–421.
[8] M. Zhu, J. Liu, Z. Lin, H. Meng, Mixed $\mathcal{H}_2/\mathcal{H}_\infty$ pitch control of wind turbine generator system based on global exact linearization and regional pole placement, Int. J. Mach. Learn. Cybern. 7 (2016) 921–930.
[9] E. Tian, Z. Wang, L. Zou, D. Yue, Chance-constrained $\mathcal{H}_\infty$ control for a class of time-varying systems with stochastic nonlinearities: the finite-horizon case, Automatica 107 (2019) 296–305.
[10] M. Gao, L. Sheng, Y. Liu, Z. Zhu, Observer-based $\mathcal{H}_\infty$ fuzzy control for nonlinear stochastic systems with multiplicative noise and successive packet dropouts, Neurocomputing 173 (2016) 2001–2008.
[11] H. Khatibi, A. Karimi, $\mathcal{H}_\infty$ controller design using an alternative to Youla parameterization, IEEE Trans. Autom. Control 55 (2010) 2119–2123.
[12] W. Sun, H. Gao, O. Kaynak, Finite frequency $\mathcal{H}_\infty$ control for vehicle active suspension systems, IEEE Trans. Control Syst. Technol. 19 (2011) 416–422.
[13] G. Wang, C. Chen, S. Yu, Robust non-fragile finite-frequency $\mathcal{H}_\infty$ static output-feedback control for active suspension systems, Mech. Syst. Signal Process. 91 (2017) 41–56.
[14] D. Zhao, S.X. Ding, H.R. Karimi, Y. Li, Y. Wang, On robust Kalman filter for two-dimensional uncertain linear discrete time-varying systems: a least squares method, Automatica 99 (2019) 203–212.
[15] D. Zhao, S.X. Ding, H.R. Karimi, Y. Li, Robust $\mathcal{H}_\infty$ filtering for two-dimensional uncertain linear discrete time-varying systems: a Krein space-based method, IEEE Trans. Autom. Control 64 (2019) 5124–5131.
[16] Y. Liu, B. Guo, J.H. Park, S. Lee, Nonfragile exponential synchronization of delayed complex dynamical networks with memory sampled-data control, IEEE Trans. Neural Networks Learn. Syst. 29 (2018) 118–128.
[17] H. Gao, W. Sun, P. Shi, Robust sampled-data $\mathcal{H}_\infty$ control for vehicle active suspension systems, IEEE Trans. Control Syst. Technol. 18 (2010) 238–245.
[18] C. Ge, J.H. Park, C. Hua, X. Guan, Nonfragile consensus of multiagent systems based on memory sampled-data control, IEEE Trans. Syst. Man Cybern. Syst. (2018) 1–9.
[19] H. Li, X. Jing, H. Lam, P. Shi, Fuzzy sampled-data control for uncertain vehicle suspension systems, IEEE Trans. Cybern. 44 (2014) 1111–1126.
[20] L. Hetel, C. Fiter, H. Omran, A. Seuret, E. Fridman, J.-P. Richard, S.I. Niculescu, Recent developments on the stability of systems with aperiodic sampling: an overview, Automatica 76 (2017) 309–335.
[21] S.H. Lee, M.J. Park, O.M. Kwon, R. Sakthivel, Advanced sampled-data synchronization control for complex dynamical networks with coupling time-varying delays, Inf. Sci. 420 (2017) 454–465.
[22] X.-M. Zhang, Q.-L. Han, Output feedback stabilization of networked control systems with a logic zero-order-hold, Inf. Sci. 381 (2017) 78–91.
[23] C. Peng, Y.-C. Tian, Delay-dependent robust $\mathcal{H}_\infty$ control for uncertain systems with time-varying delay, Inf. Sci. 179 (2009) 3187–3197.
[24] J.-H. Kim, Further improvement of Jensen inequality and application to stability of time-delayed systems, Automatica 64 (2016) 121–125.
[25] C.-K. Zhang, Y. He, L. Jiang, et al, Stability analysis of systems with time-varying delay via relaxed integral inequalities, Syst. Control Lett. 92 (2016) 52–61.
[26] P. Park, J.W. Ko, C. Jeong, Reciprocally convex approach to stability of systems with time-varying delays, Automatica 47 (2011) 235–238.
[27] C.-C. Chen, Z.-Y. Sun, A unified approach to finite-time stabilization of high-order nonlinear systems with an asymmetric output constraint, Automatica 111 (2020) 108581.
[28] K. Liu, A. Seuret, Comparison of bounding methods for stability analysis of systems with time-varying delays, J. Franklin Inst. 354 (2017) 2979–2993.
[29] J.H. Park, T.H. Lee, Y. Liu, J. Chen, Dynamic systems with time delays, Stab. Control (2019).
[30] C.-K. Zhang, Y. He, L. Jiang, M. Wu, Q.-G. Wang, An extended reciprocally convex matrix inequality for stability analysis of systems with time-varying delay, Automatica 85 (2017) 481–485.
[31] A. Seuret, K. Liu, F. Gouaisbaut, Generalized reciprocally convex combination lemmas and its application to time-delay systems, Automatica 95 (2018) 488–493.
[32] H. Li, Sampled-data state estimation for complex dynamical networks with time-varying delay and stochastic sampling, Neurocomputing 138 (2014) 78–85.
[33] L. Fang, L. Ma, S. Ding, D. Zhao, Finite-time stabilization for a class of high-order stochastic nonlinear systems with an output constraint, Appl. Math. Comput. 358 (2019) 63–79.
[34] X. Wu, Y. Tang, W. Zhang, Stability analysis of stochastic delayed systems with an application to multi-agent systems, IEEE Trans. Autom. Control 61 (2016) 4143–4149.
[35] H. Gao, J. Wu, P. Shi, Robust sampled-data $\mathcal{H}_\infty$ control with stochastic sampling, Automatica 45 (2009) 1729–1736.
[36] H. Dong, Z. Wang, S.X. Ding, H. Gao, Event-based $\mathcal{H}_\infty$ filter design for a class of nonlinear time-varying systems with fading channels and multiplicative noises, IEEE Trans. Signal Process. 63 (2015) 3387–3395.
[37] J. Liang, Z. Wang, Y. Liu, X. Liu, State estimation for two-dimensional complex networks with randomly occurring nonlinearities and randomly varying sensor delays, Int. J. Robust Nonlinear Control 24 (2014) 18–38.
[38] E. Tian, D. Yue, C. Peng, Reliable control for networked control systems with probabilistic sensors and actuators faults, IET Control Theory 4 (2010) 1478–1488.
[39] Y. Wang, W. Zhou, J. Luo, H. Yan, H. Pu, Y. Peng, Reliable intelligent path following control for a robotic airship against sensor faults, IEEE/ASME Trans. Mechatron. 24 (2019) 2572–2582.
[40] K. Schenk, B. Gülbitti, J. Lunze, Cooperative fault-tolerant control of networked control systems, IFAC-PapersOnLine 51 (2018) 570–577.
[41] S. Vimal Kumar, R. Raja, S. Marshal Anthoni, J. Cao, Z. Tu, Robust finite-time non-fragile sampled-data control for T-S fuzzy flexible spacecraft model with stochastic actuator faults, Appl. Math. Comput. 321 (2018) 483–497.
[42] R. Manivannan, R. Samidurai, J. Cao, M. Perc, Design of resilient reliable dissipativity control for systems with actuator faults and probabilistic time-delay signals via sampled-data approach, IEEE Trans. Syst. Man Cybern. Syst. (2018) 1–13.
[43] Y. Wang, H.R. Karimi, H. Lam, H. Yan, Fuzzy output tracking control and filtering for nonlinear discrete-time descriptor systems under unreliable communication links, IEEE Trans. Cybern. (2019) 1–11.

[44] Y. Wang, X. Yang, H. Yan, Reliable fuzzy tracking control of near-space hypersonic vehicle using aperiodic measurement information, IEEE Trans. Ind. Electron. 66 (2019) 9439–9447.
[45] W. Zhang, Q.-L. Han, Y. Tang, Y. Liu, Sampled-data control for a class of linear time-varying systems, Automatica 103 (2019) 126–134.
[46] E. Tian, D. Yue, C. Peng, Reliable control for networked control systems with probabilistic actuator fault and random delays, J. Franklin Inst. 347 (2010) 1907–1926.
[47] A. Seuret, F. Gouaisbaut, Hierarchy of LMI conditions for the stability analysis of time-delay systems, Syst. Control Lett. 81 (2015) 1–7.
[48] G. Wang, M. Chadli, H. Chen, Z. Zhou, Event-triggered control for active vehicle suspension systems with network-induced delays, J. Franklin Inst. 356 (2019) 147–172.
[49] H. Li, X. Jing, H.R. Karimi, Output-feedback-based H_∞) control for vehicle suspension systems with control delay, IEEE Trans. Ind. Electron. 61 (2014) 436–446.